Please fill in the name of the event you are preparing this manuscript for.	SPE Improved Oil Recovery Conference
Please fill in your 6-digit SPE manuscript number.	SPE-200324-MS
Please fill in your manuscript title.	Stability and Behavior in Carbonate Cores for New EOR Polymers at Elevated Temperatures in Hard Saline Brines

Please fill in your author name(s) and company affiliation.

Given Name	Surname	Company
Randall S.	Seright	New Mexico Tech
Kathryn E.	Wavrik	New Mexico Tech
Guoyin	Zhang	New Mexico Tech
Abdulkareem M.	AlSofi	Saudi Aramco

Abstract

The goal of this work was to identify viable polymers for use in polymer flooding high-temperature carbonate reservoirs with hard, saline brines. This study extensively examined recent EOR polymers for stability, including new ATBS polymers with a high degree of polymerization, scleroglucan, NVP-based polymers, and hydrophobic associative polymers. For each polymer, stability experiments were performed over a two-year period under oxygen-free conditions (less than one parts per billion, ppb or ~µg/L) at various temperatures up to 180°C in brines with total dissolved solids (TDS) ranging from 0.69% to 24.4%, including divalent cations from 0.034% to 2.16%. Use of Arrhenius analysis was a novel feature of this work. This rarely-used method allows relatively rapid assessment of the long-term stability of EOR polymers. Rather than wait years or decades for results from conventional stability studies at the reservoir temperature, reliable estimates of the time-temperature stability relations were obtained within two years. Arrhenius analysis was used to project polymer viscosity half-lives at the target reservoir temperature of 99°C. The analysis suggests that a set of ATBS polymers will exhibit a viscosity half-life over 5 years at 120°C and over 50 years at 99°C—representing a novel finding of this work and a major advance for extending polymer flooding to higher temperatures.

For five polymers that showed potential for application at higher temperatures, corefloods were performed under anaerobic conditions. Another novel feature of this work was that anaerobic floods were performed without using chemical oxygen scavengers, chemical stabilizing packages, or chelating agents (that are feared to alter rock properties). Using carbonate cores and representative conditions, corefloods were performed to evaluate polymer retention, rheology in porous media, susceptibility to mechanical degradation, and residual resistance factor for each of the polymers at 99°C.

Introduction

A significant fraction of the oil that could be recovered by polymer flooding and other chemical flooding methods exists in hot carbonate reservoirs (Masalmeh *et al*. 2019). When common concentrations of divalent cations are present in a brine (5-10% of the total salinity), HPAM polymers eventually hydrolyze and precipitate in hot reservoirs—compromising their utility above 70°C (Davison and Mentzer 1982, Zaitoun and Potie 1983, Moradi-Araghi and Doe 1987, Ryles 1988). If no dissolved oxygen or divalent cations are present, HPAM solutions can exhibit a viscosity half-life of eight years at 100°C and two years at 120°C (Seright *et al.* 2010). If large amounts of soft water are available, HPAM solutions could (in concept) be effective in reservoirs up to 100°C if the polymer bank is sufficiently viscous to sweep through the reservoir with minimum mixing with the hard formation water (Maitin 1992, Seright *et al.* 2010). This concept requires control of ion exchange and carbonate dissolution so that too much hardness is not added to the polymer bank by interaction with formation minerals (Pope *et al.* 1978; Lake 1989, Berge *et al.* 2018). Berge *et al.* 2018 extensively examined ion exchange in the presence of HPAM, demonstrating that the polymer promotes dissolution of divalent cations.

However, in cases where use of soft water is impractical, more stable polymers are needed for applications in reservoirs that are hotter than 70°C. Since the 1980s, more stable synthetic polymers have been made by incorporating vinylpyrrolidone (NVP) and AMPS or ATBS into acrylamide-based polymers (Doe *et al.* 1987, Moradi-Araghi *et al.* 1987). Until recently, issues with cost-effectiveness limited their application (because of higher monomer cost and lower degree of polymerization than HPAM).

Within the past few years, polymer manufactures have proposed and evaluated several new or improved polymers for EOR use at elevated temperatures (Reichenbach-Klinke *et al*. 2011, 2013,2018; Gaillard *et al*. 2010, 2014, 2015; Vermolen *et al*. 2011; Leonhart *et al*. 2014; Siggel *et al*. 2014; AlZahid *et al*. 2016; Leblanc *et al*. 2015; Dupuis *et al*. 2017; Drivers *et al*. 2017; Jensen *et a*l. 2018; Rodriguez *et al*. 2018a,b). Some recent work with these polymers has been reviewed by Al Fazazi *et al*. (2018) and Delamaide (2018). Our paper examines the most promising polymers for potential use in high-temperature, high-salinity reservoirs with large spacing. Specifically, the envisioned application is a carbonate reservoir at 99°C, with formation salinity of 24.4%-TDS (total dissolved solids). Less saline waters could be available for injection (i.e., "Injection" water with 6.9%-TDS salinity and "Smart" water with 0.69%-TDS salinity), but all have significant concentrations of divalent cations. The application shall rely on well spacings that are 1-2 km. With 1 km spacing, the inter-well polymer transit time is expected to be around 17 years. For a polymer or chemical flooding process to be effective, the polymer must be sufficiently stable for a significant fraction of the expected inter-well transit time. To clarify, a 17-year transit time is approximated by dividing the average aqueous-phase pore volume in a pattern at residual oil saturation by the average injection rate. Of course, if the injected polymer channels inefficiently through the reservoir (e.g., through fractures), the actual inter-well transit time may be less. However, a prudent design would mitigate severe channeling before proceeding with the polymer flood.

The largest well spacing for existing field applications of polymer flooding is around 300 meters (Wassmuth *et al*. 2007, Wang *et al*. 2008, 2009). So, one may question the viability of using a well spacing of 1-2 km. A reduced well spacing could significantly speed up response to the polymer flood and reduce the stability requirement for the polymer. However, for the target application, the operator has proprietary technical and economic reasons for insisting on large spacings.

Previous studies of polymer stability at elevated temperature were commonly performed at the temperature of the target reservoir (e.g., Shupe 1981, Yang and Treiber 1985, Jabbar *et al*. 2017,2018). Unfortunately, very few of these studies continued for more than two years. If the anticipated inter-well transit time is large compared to the life of the stability study, these studies cannot be expected to make credible predictions of polymer long-term effectiveness. To overcome this limitation, Arrhenius analyses can be employed. By performing stability studies at a number of elevated temperatures, the Arrhenius analysis can establish the relation between viscosity, time, and temperature. Then, the Arrhenius equation can project polymer stability (e.g., viscosity half-life) at the target reservoir temperature. This approach was successfully used in two previous studies—one with xanthan (Seright and Henrici 1990) and one with HPAM with no divalent cations present (Seright *et al.* 2010. The primary criticism of the Arrhenius method is that predictions may be compromised if the mechanism of polymer degradation changes over the temperature range of the study (i.e., between the reservoir temperature to the maximum temperature of the study). However, Swiecinski *et al*. (2016), Sandengen *et al.* (2017, 2018) and Nurmi *et al*. (2018) recently examined the Arrhenius analysis for acrylamide-ATBS-based polymers and suggested that the method appeared valid.

This work will first provide a literature review of EOR polymer stability at elevated temperatures. The goals of this literature review are (1) to introduce the reader to previous stability studies of EOR polymers in the absence of dissolved oxygen, (2) to point out that most previous studies occurred only at the temperature of the intended application and occurred for a short time (two years or less), and (3) to provide an understanding of why most previous polymers (especially acrylamide-based polymers) were not sufficiently stable for high-temperature EOR applications. After the literature review, we detail the experimental methodology and the application of the Arrhenius analysis in assessing stability of EOR polymers. Although the Arrhenius analysis is not new to reaction kinetics, the petroleum literature has very few reports directed at EOR polymer stability (Seright and Henrici 1990; Seright *et al*. 2010). Without the Arrhenius analysis, reliable studies of polymer stability require many years or decades to perform.

In our research, the Arrhenius analysis assumes that the mechanism of polymer degradation remains basically unchanged over the temperature range of the study. Mechanisms envisioned for degradation for synthetic polymers include (1) oxidative degradation, (2) hydrolysis of side groups, followed by precipitation with divalent cations, (3) crosslinking/gelation associated with side groups reacting with multivalent cations, and (4) breakage of the polymer backbone by some other mechanism. For biopolymers, the envisioned mechanisms are much the same, although hydrolysis of side groups is unlikely to cause significant viscosity loss, while hydrolysis of the polysaccharide backbone is important (Seright and Henrici 1990). Because our studies were conducted in the complete absence of dissolved oxygen, oxidative degradation is eliminated as a mechanism. For polymers that have a moderate or high acrylamide or acrylate composition, the literature indicates that the dominant degradation mechanism (in the absence of oxygen) is hydrolysis of side groups, followed by precipitation with divalent cations. Our stability studies will confirm this finding. For synthetic polymers that have a low (or zero) acrylamide/acrylate content, we hope/speculate that the mechanisms of hydrolysis/precipitation/gelation will be minimized—leaving thermal breaking of the polymer backbone as the single/dominant mechanism for viscosity loss. With a lesser number of mechanisms available for degradation, the Arrhenius analysis becomes more viable for long-term projections. In our experimental work, these ideas will be examined during long-term stability tests of the most promising EOR polymers. Stability tests were performed at four elevated temperatures (120°C, 140°C, 160°C, and 180°C) and then the Arrhenius analysis established the relation between viscosity, time, and temperature. Ultimately, the Arrhenius equation will project polymer stability (e.g., viscosity half-life) at the target reservoir temperature of 99°C. In contrast to studies with xanthan (Seright and Henrici 1990) and HPAM with no divalent cations present (Seright *et al.* 2010), the current study examines relatively new polymers in the presence of significant levels of divalent cations.

For five polymers that showed potential for application at higher temperatures, in addition to stability studies, this work also performed corefloods under anaerobic conditions. A procedure was developed to perform these floods with continuously monitored dissolved oxygen concentrations, typically below 5 ppb (μg/L). This was done without using chemical oxygen scavengers, chemical stabilizing packages, or chelating agents (that are feared to alter rock properties). Using representative carbonate cores and conditions, corefloods were performed to evaluate polymer retention, rheology in porous media, susceptibility to mechanical degradation, and residual resistance factor at 99°C.

Literature Review of EOR Polymer Stability at Elevated Temperatures

Degradation Mechanisms for Synthetic Polymers. At elevated temperatures, acrylamide-based polymers experienced degradation by at least three different mechanisms: (1) amide/side-group hydrolysis, followed by precipitation with divalent cations, (2) reaction with dissolved oxygen (resulting in cleavage of the C-C backbone), and (3) breakage of the C-C backbone by some mechanism that does not involve dissolved oxygen. The literature on oxidative degradation of EOR polymers has been extensively reviewed elsewhere (e.g., Seright and Skjevrak 2015, Jouenne *et al.* 2017). Achieving less than 20-ppb dissolved oxygen is straight-forward for most field applications where subsurface waters are used for polymer make-up (Seright and Skjevrak 2015). Prudent engineering of surface equipment and leak prevention allows maintenance of near-zero dissolved oxygen levels in the flow-stream (Seright and Skjevrak 2015). For the low levels of dissolved oxygen that remain, contact with the reducing environment of a reservoir will quickly remove all dissolve oxygen (although some polymer degradation can be expected in hot reservoirs before the oxygen is depleted) (Seright *et al*. 2010). Polymer stability results described in Seright and Henrici (1990) and Seright *et al*. (2010) were dominantly conducted without using chemical oxygen scavengers and "stabilization packages" (i.e., only non-chemical methods were used to remove oxygen), and yet (as described in those papers) they reported the greatest stability for xanthan and HPAM of any study to date. As noted by Seright and Skjevrak (2015), chemical oxygen scavangers and "stabilization packages" are only of value if significant dissolved oxygen is present. Seright *et al*. (2010) noted that even if ambient levels of dissolved oxygen are present (3-8 parts per million, ppm or ~mg/L), the highly reducing conditions and iron minerals (e.g., pyrite, siderite) in an oil reservoir will usually consume that oxygen within hours or days, even at low temperature (Xu *et al*. 2000). Since our studies were performed in the absence of dissolved oxygen, this topic will not be discussed further.

Side-Group Hydrolysis. HPAM polymers are known to be unstable at elevated temperatures if divalent cations are present (Davison and Mentzer 1982; Zaitoun and Potie 1983; Moradi-Araghi and Doe 1987; Ryles 1988). For temperatures greater than 60°C, even at neutral pH, acrylamide groups within the HPAM polymer experience hydrolysis to form acrylate groups. If significant concentrations of divalent cations (especially Ca^{2+}) are present, HPAM polymers can precipitate if the fraction of acrylate groups (i.e., the degree of hydrolysis) in the polymer becomes too high. These facts limit the utility of HPAM polymers for many potential EOR applications in warmer reservoirs. Moradi-Araghi and Doe (1987) suggested hardness limits in brines for various temperatures: 2,000 mg/L for 75°C, 500 mg/L for 88°C, and 270 mg/L for 96°C. For brines containing less than 20 mg/L divalent cations, they suggest that polymer hydrolysis and precipitation will not be a problem for temperatures of 204°C or greater.

For the work in our paper, three brines were used: (1) Connate water, (2) Injection water, and (3) Smart water. Connate water contained 180.5 g/L NaCl, 69.99 g/L $CaCl_2*2H_2O$, and 21.4 g/L $MgCl_2*6H_2O$ (243.571 g/L TDS). Injection water contained 58.296 g/L NaCl, 10.56 g/L $CaCl_2*2H_2O$, and 4.48 g/L $MgCl_2*6H_2O$ (68.975 g/L TDS). Smart water contained 5.5782 g/L NaCl, 1.0564 g/L $CaCl_2*2H_2O$, 0.4116 g/L $MgCl_2*6H_2O$, 0.2617 g/L Na_2SO_4, and 0.05099 g/L $NaHCO_3$ (6.898 g/L TDS). All brines were filtered through 0.45 μm filters before use. Table 1 summarizes the water compositions used in this work.

Table 1—Water compositions (g/L)

Water:	Smart	Injection	Connate
Na	2.293	22.928	70.991
Ca	0.288	2.880	19.080
Mg	0.054	0.536	2.561
SO_4^{2-}	0.177	0	0
HCO_3^-	0.037	0	0
TDS	6.898	68.975	243.571

The hardness limit (from Moradi-Araghi and Doe) of 270 mg/L for 96°C suggests that even the Smart water has too much calcium (288 mg/L) to avoid the hydrolysis/precipitation problem for normal HPAM polymers at 99°C. The limit proposed by Moradi-Araghi and Doe assumed that half the divalent ion content was calcium and the other half was magnesium. Calcium is known to be much more active than magnesium in precipitating polymers (Moradi-Araghi and Doe 1987). Consequently, significant HPAM loses can be expected due to hydrolysis/precipitation at 99°C in all brines studied in this work.

Consideration has been given to the rate of amide hydrolysis in HPAM polymers. Data from Moradi-Araghi and Doe (1987) indicate that in 5% NaCl solution at 90-100°C, 60% degree of hydrolysis will be reached after 20-30 days. Depending on the temperature and divalent ion concentration, HPAM precipitation can be anticipated by the time 60% degree of hydrolysis is reached.

Examination of the literature indicates that the rate of amide hydrolysis is accelerated by the presence of neighboring acrylate groups (Swiecinski *et al*. 2016, Sandengen *et al*. 2017, 2018). However, for a given pH, similar kinetics are followed up to about 55% degree of hydrolysis. That suggests that for practical field applications, HPAM will probably end up with the same degree of hydrolysis deep in a 99°C reservoir, regardless of the HPAM chosen (i.e., Mw, copolymerized, post-hydrolyzed, initial acrylamide-acrylate sequence, etc.). Certain additives can affect the cloud point (temperature where HPAM becomes turbid from the phase transition), but these additives will probably be diluted or stripped before the polymer reaches very far into the reservoir. Thus, any commercially available HPAM is expected to experience hydrolysis and precipitation in the three brines for our current work. The most obvious method to make HPAM viable in these brines at 99°C is to reduce the divalent cation content (especially calcium) below 130 mg/L.

Polymer precipitation can be overcome by copolymerizing acrylamide with more-stable monomers (such as AMPS/ATBS or N-vinylpyrrolidone) that resist hydrolysis (Doe *et al*. 1987, Moradi-Araghi *et al*. 1987, Gaillard *et al*. 2010, Gaillard *et al*. 2014, Gaillard *et al*. 2015, Rodriguez *et al*. 2016,2018, Drivers *et al*. 2017, Dupuis *et al*. 2017, Zhang *et al*. 2017). These polymers have significantly improved resistance to precipitation; however, they are noticeably more expensive and less efficient viscosifiers than HPAM. Incidentally, our understanding is that AMPS (2-acrylamido-2-methylpropanesulfonic acid) and ATBS (2-acrylamido-tertbutylsulfonic acid) are synonyms for the same molecule.

Sandengen *et al*. (2017) studied the rates of acrylamide and ATBS hydrolysis for different acrylamide/ATBS copolymers. For initial ATBS content from 15-35% (i.e., 65-85% acrylamide), the number of acrylamide groups in the polymers decreased to 30% after 140 days at 100°C and to 5% after 60 days at 120°C (with the acrylamide being converted to acrylate). The half-life for ATBS hydrolysis was about 20 days at 120°C (when the initial ATBS content was 15-35%). ATBS hydrolysis was not apparent at 80°C, so the question is open whether ATBS hydrolysis will be significant at 100°C for a practical EOR time frame (e.g., 5 years). Our interpretation/extrapolation from this work is that the hydrolysis/precipitation problem (at 99°C in our three brines) cannot be avoided for ATBS (AMPS) contents below 40-50% (in the polymer).

Even if ATBS is used, there is uncertainty as to whether ATBS will be hydrolyzed significantly over five years at 99°C (Parker and Lezzi 1993). Sandengen *et al*. (2018) studied stability of copolymers with up to 80% ATBS at temperatures of 120°C and 140°C. For a polymer with 70% ATBS in synthetic seawater, the viscosity half-life was about 50 days at 120°C and 5.9 times faster at 140°C. If this trend is extrapolated to 100°C, the 70% ATBS polymer is projected to have a viscosity half-life around 300 days. Sandengen *et al*. (2018) found that a polymer with 80% ATBS exhibited a viscosity half-life at 140°C that was four times longer than for a polymer with 70% ATBS. Extrapolating this trend suggests that a polymer requires at least 80% ATBS to provide a viscosity half-life longer than three years at 100°C. Of course, one can hope that this projection is pessimistic for 100°C. But note the comment of Sandengen *et al*. (2018): ATBS and acrylamide hydrolysis reactions "do not reach some equilibrium condition with remaining AM or ATBS." Thus, acrylamide-ATBS co-polymers are expected to eventually hydrolyze to acrylate extensively at elevated temperatures.

A particularly useful observation from Sandengen *et al*. (2017) was that Arrhenius analysis (judging polymer stability from tests performed at various temperatures above the target temperature) was valid for HPAM-type polymers. Sandengen *et al*. (2018) also suggested that the rate of hydrolysis was not sensitive to total salinity.

A detailed examination was performed of several previous studies of stability of polymers for high-temperature EOR applications, including those from Doe *et al*. (1987), Vermolen *et al*. (2011), Gaillard *et al*. (2014), Zhuoyan *et al*. (2015), Gaillard *et al*. (2015), Dupuis *et al*. (2017), and Rodriquez *et al*. (2018). This examination revealed that most previous studies (1) occurred at only at the temperature of the intended application, (2) occurred for a short time (two years or less), and (3) were consistent with the points made in the previous section—that high concentrations of stable monomers must be incorporated to improve stability of synthetic EOR polymers.

Degradation Mechanisms for Polysaccharides. Polysaccharides (xanthan, scleroglucan, diutan, schizophyllan) are known to experience degradation by (1) oxidation and (2) hydrolysis. A literature review of these mechanisms (focused on xanthan degradation) was provided by Seright and Henrici (1990). They noted that in the absence of dissolved oxygen, xanthan solutions exhibit their maximum stability at pH values between 7 and 8. Below pH 7, viscosity decay constants decrease significantly with decreasing pH, indicating that acid-catalyzed hydrolysis may have an important role in xanthan degradation. Xanthan stability also drops sharply above pH 8 as solutions become more alkaline, suggesting that base-catalyzed fragmentation reactions may also be important. Their analysis indicated that under ideal conditions (no dissolved oxygen, pH 7 to 8, moderate to high salinities), a xanthan solution could maintain at least half of its original viscosity for a period of 5 years if the temperature does not exceed 75 to 80°C. Thus, xanthan was not deemed sufficiently stable for application at 99°C.

Some studies of stability of other EOR polysaccharides (scleroglucan, diutan, schizophyllan) suggest that these polymers have potential for application at higher temperatures. Jensen *et al.* (2018) reported insignificant viscosity loss for a scleroglucan biopolymer (in seawater) after one year of storage at 95ºC. Also, in synthetic seawater, Davidson and Mentzer (1982) and Kalpakci *et al*. (1990) reported good stability for scleroglucan. In particular, Kalpakci *et al*. reported little or no viscosity loss for scleroglucan solutions over 720 days at 100°C. In contrast, Ryles (1988) noted that scleroglucan degraded within three months at 90°C. However, the stability of these polymers has not been examined using the Arrhenius analysis. Biodegradation is beyond the scope of this study.

Experimental Procedures

Long-Term Stability Studies

Polymers. During this work, 22 polymer candidates were examined from 14 companies. However, this paper will focus on the polymers that exhibited the greatest potential for stability at elevated temperatures. All polymers discussed in this paper are commercially available. Table 2 provides a listing of the polymers examined. The first column lists our non-commercial code for a given polymer. The second column lists the polymer concentration (in mg/L or ppm) to achieve about 25 cp (at 25°C, 7.3 s^{-1}) in Injection water (6.9% TDS with 0.288% Ca and 0.0536% Mg). The third column provides what is publicly known about composition of these polymers, while the fourth column indicates that all polymers were provided in powder form. Gaillard *et al*. (2014), Dupuis *et al*. (2017), and Rodriquez *et al*. (2018) provide good discussions of the relative cost-effectiveness of polymers containing ATBS and NVP. Generally, the relative cost for a given synthetic polymer in Table 2 increases linearly with increased polymer concentration. It will also increase with increased ATBS content, and especially with increased NVP content.

Table 2—Polymers examined.

Polymer code	mg/L to achieve ~25 cp in 6.9% -TDS water	Polymer composition	Product form
HPAM6	1600	30% acrylate, 70% acrylamide, 18 million g/mol	powder
AAMPS1	2750	25% ATBS, 75% acrylamide, 10-12 million g/mol	powder
ATBSA	4100	>90% ATBS	powder
ATBSB	2900	>90% ATBS, higher Mw	powder
ATBST	3500	>90% ATBS, thermoresponsive	powder
ATBS8A	3500	~80% ATBS	powder
ATBS8B	2700	~80% ATBS	powder
AMNVPATBS1	4400	50-65% acrylamide, 20-25% ATBS, 5-20% NVP, 3-5 million g/mol	powder
NVP1	9000	Large % NVP	powder
HYASA	8000	Large % unspecified stable monomer, small % hydrophobic associative monomer	powder
HYASB	8000	Large % unspecified stable monomer, small % hydrophobic associative monomer	powder
SG1	950	scleroglucan	powder

Stability Methodology. The viscosity targeted for the studies was 20-30 cp at 7.3 s^{-1}, 25°C. Much of our methodology for assessing polymer stability can be found in Seright and Henrici (1990), Seright *et al.* (2010), and Seright and Skjevrak (2015). Polymer samples were prepared and viscosities, pH values, and dissolved oxygen levels were measured inside an anaerobic chamber (Forma Scientific Model 1025™). Figure 1 shows one of these chambers. This unit continuously circulated an anaerobic gas (10-15% hydrogen and 85-90% nitrogen) through a palladium catalyst and a desiccant. Any free oxygen was reacted with hydrogen to form water, which was removed by the desiccant. Oxygen measurements were made with either a colorimetric metric method (CHEMET™ with a limit of oxygen detection between 1 and 5 ppb in aqueous solution) or a very sensitive dissolved oxygen meter [PreSens Fibox 4 Trace, which is sensitive to 1 ppb (μg/L) oxygen in the liquid phase]. Under most circumstances, measurements indicated 0.000% oxygen in our chamber gas. As an exception, the chamber gas could rise to 0.035% oxygen immediately after moving items into the anaerobic chamber from the transfer chamber. As such, when anything was brought in from outside the main chamber, the transfer chamber was purged twice with pure nitrogen gas and once with our anaerobic gas, interspersed with evacuations to 65 kPa vacuum. Within 45 minutes of making a transfer, the oxygen content in the main chamber returned to 0.000%. Polymer solutions that were prepared in the anaerobic chamber typically contained no dissolved oxygen (i.e., less than 1 ppb or μg/L).

Figure 1—Anaerobic chamber.

Brines were mixed and filtered through 0.45 μm Millipore filters outside the anaerobic chamber. Then the brine was moved into the chamber, and a pump was used to bubble anaerobic gas through the brine. Less than 1 hour was required to drive the dissolved oxygen content below 1 μg/L. A vortex was formed using a magnetic stirrer and powder-form synthetic polymer was added in the traditional manner and then mixed overnight at low speed. Note that the powder-form polymers were stored inside the anaerobic chamber. Scleroglucan was mixed using a blender inside the anaerobic chamber. Polymer solution viscosities were measured inside the anaerobic chamber at 7.3 s^{-1} and room temperature using a Brookfield Model DV-E™ viscometer with a UL adapter. After preparation, 70 cm^3 of polymer solution were placed in a 150-cm^3 stainless steel cylinder and sealed using stainless steel plugs with blemish-free threads that were wrapped with yellow 3.5 mil gas-lineTeflon tape. Normal white Teflon tape was inadequate. Then the cylinders were removed from the anaerobic chamber and placed in silicone oil baths (e.g., Thermo Neslab EX7™) for various times at different temperatures ranging from 99 to 180ºC. When a viscosity measurement was to be made, the cylinder was removed from the silicone bath, cooled rapidly in an ice bath, and then brought into the anaerobic chamber for viscosity, oxygen, and pH measurements at room temperature. After the measurements, the sample was returned to the same cylinder, resealed, removed from the anaerobic chamber, and returned to the appropriate silicone bath. An advantage of this method over previous flame-sealed glass-ampoule methods is that all measurements over time were made on the same polymer solution sample. Also, pH and dissolved oxygen measurements could readily be made on these samples. A disadvantage is that if the seal is compromised for the sample cylinders, the entire sample is lost. Fortunately, the technique has been perfected so that samples are rarely lost.

Illustration of Stability Data Collected. The Arrhenius method employed in this work involves examining the stability of a given polymer (in a given brine) at four elevated temperatures (120°C, 140°C, 160°C, and 180°C) and then using the Arrhenius equation to project polymer stability at lower temperatures (especially at the target temperature of 99°C). To illustrate the data collected for each polymer, Figure 2 shows the stability to date for the polymer, ATBSA, at the four elevated temperatures in Injection water and Connate water, respectively. (As mentioned earlier, after a given time of storage at a given temperature, viscosity measurements were made at 25°C and a shear rate of 7.3 s^{-1}, for consistency—explaining the conditions listed on the *y*-axes of Figure 2.) As of 621 days into the study, this polymer exhibits excellent stability in all three brines at 120°C. In all three brines, the viscosity half-life was roughly 1 year at 140°C, 50 days at 160°C and about 8 days at 180°C Achieving ~25 cp required 3100 mg/L in Smart water, 4100 mg/L in Injection water, and 4200 mg/L in Connate water. At temperatures of 140°C, 160°C, and 180°C, the studies have effectively reached completion because viscosities have decreased to low values. However, at 120°C, viscosities have not deteriorated much after 621 days. Thus, the data at 120°C must be projected to estimate the decay constant at that temperature.

In Figure 2b, note that substantial gel was noted in the Connate water after 83 days at 160°C and 467 days at 140°C. These observations suggest a change in degradation mechanism at these times and temperatures. Presumably, before these indicated storage times, the polymer degraded by thermal breaking of the polymer backbone. However, at the indicated times, viscosity loss was accelerated by the onset of gel formation. Perhaps, gel formation resulted after sufficient hydrolysis of side groups led to reaction with divalent cations in the very hard Connate water. Apparently, this did not occur for the same polymer in the Injection water (Figure 2b). One could argue that the most appropriate data to use for the Arrhenius analysis is that acquired before the onset of the gelation mechanism (in the Connate water) at a given temperature.

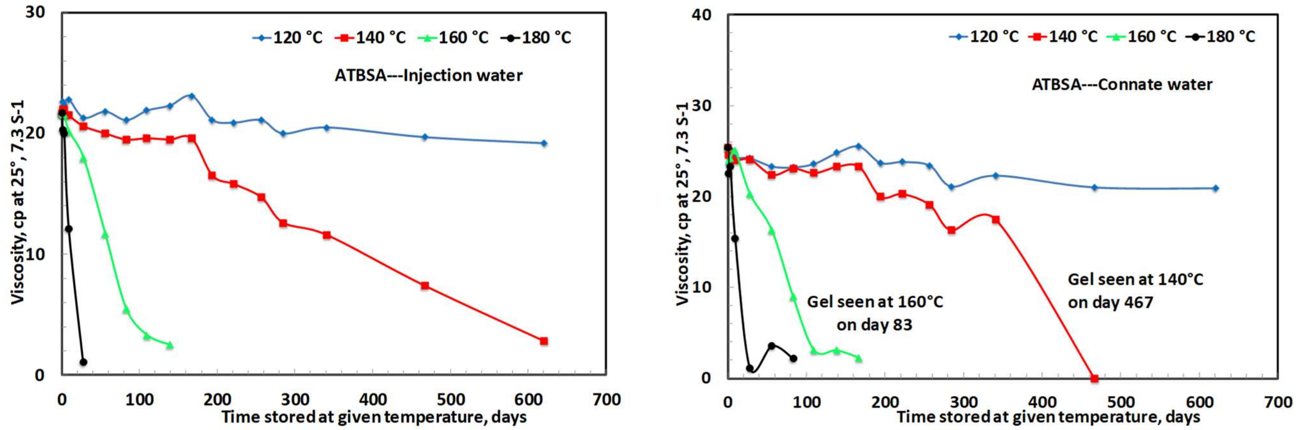

Figure 2—Stability of ATBSA: (a) 4100-mg/L in Injection water (6.9% TDS), left and (b) 4200-mg/L ATBSA in Connate water (24.4% TDS), right.

Arrhenius Projections of Polymer Stability at 99°C. The ultimate goal of this work is to estimate polymer stability at the reservoir temperature (99°C) based on experimental results obtained at higher temperatures (i.e., 120, 140, 160, 180°C). Use of the Arrhenius method allows relatively rapid collection of stability data (at several temperatures hotter than the target reservoir) and projection of polymer stability for long time periods at lower temperatures (especially at the temperature of the target reservoir). Without this method, stability studies must be conducted for a substantial fraction of the life of the field project (many years). In the Arrhenius method, stability data versus time (e.g., Figure 2) are first fitted to the equation:

$$(\mu-\mu_s)/(\mu_o-\mu_s) = A_1 \exp(-t/\tau) \quad (1)$$

where μ is viscosity at time, t, μ_s is solvent viscosity, and μ_o is original viscosity at time zero. A_1 and τ are fitting parameter. In particular, τ is the decay constant (in days) for degradation of a particular polymer solution. The τ values can be related to temperature (T) through the Arrhenius Equation:

$$1/\tau = A_2 \exp[-E/(RT)] \quad (2)$$

where E is the activation energy, R is the universal gas constant, and A_2 is a pre-exponential parameter (a constant that is individual for a given reaction and sometimes indicative of the frequency of molecular interactions). This equation was used to fit the τ values versus temperature and to project τ values at 99°C. The τ values at 99°C were then converted to projected viscosity half-lives using the equation:

$$\text{Half-life} = \tau_{99°C} \times Ln\ (2) \quad (3)$$

The right-most column of Table 4 lists projected half-lives for the various experiments, while the right-most column of Table 5 lists correlation coefficients from the fits to Equation 2. For the case of ATBSA in Injection water, Figure 3 provides a plot that illustrates how decay constants at 120-180°C are extrapolated to estimate the viscosity decay constant at 99°C.

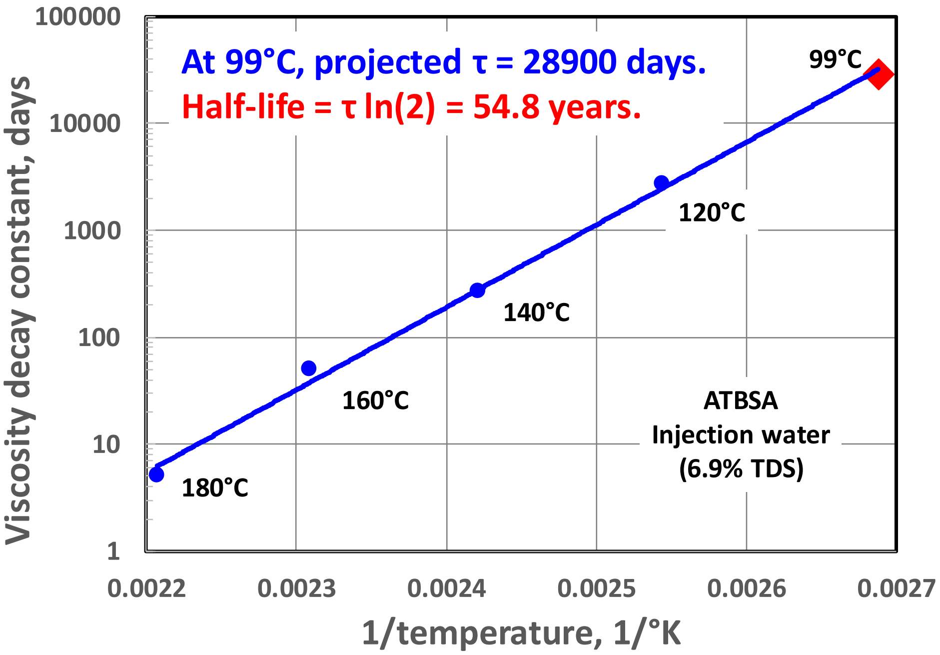

Figure 3—Projection of decay constants at high temperatures to estimate stability at 99°C.

Corefloods

Five of the polymers from the stability studies were selected for examination during anaerobic corefloods at 99°C. Even though the three ATBS polymers (ATBSA, ATBSB, and ATBST from Table 2) appear most stable from the stability studies, polymers from different suppliers were selected to increase the diversity of the examination. All corefloods were performed at 100% water saturation.

Polymers, Polymer Preparation, and Cores. Five powder-form polymers examined in this work included: (1) AMNVPATBS1 (as a benchmark), (2) ATBSA, (3) SG1 scleroglucan, (4) NVP1, and (5) HYASA. More detail for these polymers is given in Table 2 and during discussion of a given polymer.

Only Injection brine was used in the corefloods. As mentioned earlier, the brine was mixed and filtered through 0.45 μm Millipore filters outside the anaerobic chamber. Then the brine was moved into the chamber (Figure 1), and a pump was used to bubble anaerobic gas through the brine. Preparation of anaerobic polymer solutions was described earlier. Because a greater amount of fluid transfer occurred during the corefloods, the level of dissolved oxygen present (2 to 22 ppb or μg/L) was greater than during the long-term stability studies (always less than 1 μg/L).

Table 3 lists the properties of the 3.8-cm-diameter carbonate cores used in this work. Polymer concentration and viscosity (cp at 25°C and 7.3 s^{-1}) used in each core are also listed. Viscosities were measured using an AntonPaar MCR301 rheometer outside the anaerobic chamber and a Brookfield viscometer (with UL adapter) inside the anaerobic chamber. (The viscosity listings in Table 3 used the AntonPaar MRC301 rheometer.)

Table 3—Core properties and polymer concentrations for experiments.

Polymer	AMNVPATBS1	ATBSA	ATBSA	SG1	NVP1	HYASA
Core	272	28	15	264	24	324
Weight, g	118	143.0	131.8	113.2	136.3	146.7
Length, cm	5.35	6.66	6.20	5.15	6.57	6.08
k_w, md	153	145	24	106	322	504
ϕ	0.187	0.258	0.281	0.257	0.26	0.28
Concentration, mg/L	4400	4100	4100	950	9000	8000
Viscosity, cp @ 7.3 s^{-1}	20.8	21.0	22.6	34.8	20.6	26.7

Core Flood Procedures. Cores were saturated with Injection brine (68.975 g/L TDS), and porosity and initial permeability were measured under aerobic conditions. Then, cores were placed inside a CoreLab biaxial Hassler core holder and pressurized to 1300 psi (confining pressure) using anaerobic distilled water. Anaerobic fluids from inside the anaerobic chamber were piped directly into ISCO pumps. From there, the fluids were forced through the core to confirm permeability and remove any dissolved oxygen from the core. Heat tape was used to heat and maintain the core and flow lines at 99°C. Effluent from the core was piped through an ice bath (to return the fluids to near room temperature) and then back into the anaerobic chamber. Anaerobic brine was flushed through the core and back into the anaerobic chamber until the dissolved oxygen content of the effluent was less than 3 parts per billion (ppb, μg/L). With this arrangement, anaerobic core floods were performed without any chemical oxygen scavengers, chelators, or other chemicals that might change the character of the rock.

Next, for the polymer retention test, the chosen anaerobic polymer solution was piped from the anaerobic chamber into a separate ISCO pump (that had previously been made anaerobic). This polymer solution contained 20-mg/L potassium iodide (KI) as a tracer. The anaerobic polymer solution was then forced through the core at a rate of 2 ft/day (1 ft/d for the AMNVPATBS1 flood). Depending on the flood, between 11 and 21 pore volumes (PV) of polymer solution were injected, while continuously monitoring the pressure drop across the core. An ISCO Retriever 500 fraction collector was located inside the anaerobic chamber, to collect effluent samples in 3-4 cm^3 increments. Dissolved oxygen was regularly monitored during effluent collection. After collection, caps were placed on the sample tubes to prevent evaporation and to maintain oxygen-free conditions. After collection of all retention effluent samples, they were removed from the anaerobic chamber for subsequent analysis. For a given sample tube, the cap was removed, the sample was weighed, viscosity was measured using a Vilastic VE rheometer (at 25°C, 7.3 s^{-1}), and then the sample was placed back in the tube. After all the viscosities were measured, each sample was measured for KI content using a Genesys 8 spectrophotometer at a wavelength of 230 nm. Finally, the samples were analyzed for total organic carbon and nitrogen content using a Shimadzu TOC-L with TNM-L unit (for nitrogen chemiluminescence). Nitrogen content is the most reliable means to detect synthetic (HPAM-type) polymers. Total organic carbon (TOC) was used to detect polymer for SG1 scleroglucan (since the molecule does not contain nitrogen). Polymer retention values were calculated as described in Manichand and Seright (2014) and Wang *et al*. (2020).

After completion of the retention test, the polymer solution was forced through the core at a series of decreasing rates to assess rheology in porous media and susceptibility to mechanical degradation. The highest rate was used first, with the intent of achieving roughly 1000 psi across the core. This value was chosen so as not to exceed the 1300-psi confining pressure. The flow rate and pressure drop were allowed to stabilize. Then, an effluent sample was collected within the anaerobic chamber for subsequent viscosity measurement (using the Brookfield viscometer inside the chamber). Next, the injection rate was cut in half, and the process was repeated. This process was continued until the pressure drops were too low to measure reliably. The range of Darcy velocities extended from 139 ft/d down to 0.017 ft/d for AMNVPATBS1 in 153-mD rock, from 88 ft/d down to 0.4 ft/d for ATBSA in 145-mD rock, from 10.6 ft/d down to 0.16 ft/d for ATBSA in 24-mD rock, from 280 ft/d to 0.5 ft/d for SG1 scleroglucan in 106-mD rock, from 528 ft/d down to 1 ft/d for NVP1 in 322-mD rock, and from 846 ft/d down to 0.2 ft/d for HYASA in 504-mD rock. The velocity ranges were determined by polymer rheology, core permeability, the 1000-psi upper pressure limit, and lower-pressure-limit accuracy for the transducers.

After completion of the rheology/mechanical-degradation study, 1.5 liters (78-134 PV) of brine were injected and a residual resistance factor was measured.

RESULTS

Long-Term Stability Studies

The middle columns of Table 4 list τ values (viscosity decay constants in days, associated with Eq. 1) for various experiments (primarily those polymers with the greatest stability from this study), while Table 5 lists correlation coefficients from the fits to Equation 1. In examining Tables 4 and 5, note that correlation coefficients are lowest (worst) for cases where the polymer is still early in the study life (where the polymer solution has not lost much viscosity yet)—such as the ATBS polymers at 120°C. Naturally, the correlation coefficients will rise and confidence in the 99°C projections will increase as a given study matures. An indication of the reproducibility of the results in Table 4 is implied by the consistency of the decay constants and projected viscosity half-lives in the three brines for the polymers: ATBSA, ATBSB, ATBST. Since all three of these polymers have nearly the same composition (more than 90% ATBS), similar stability results were expected—as observed. Additional evidence of the reliability of projections is indicated by the correlation coefficients in Table 5.

Table 4—τ values (days from Eq. 1 fit) and 99°C half-life projections (years from Eq. 2 fit).

Polymer	Concentration, mg/L	Water / TDS	120ºC τ, days	140ºC τ, days	160ºC τ, days	180ºC τ, days	Projected half-life at 99°C, years
ATBSA	3100	Smart / 0.69%	2595	266	40	5	61.1
ATBSA	4100	Injection / 6.9%	2691	266	50	5	54.8
ATBSA	4200	Connate / 24.4%	1947	400	37	9	67.3
ATBSB	2700	Smart / 0.69%	3942	350	30	6	63.1
ATBSB	2900	Injection / 6.9%	3990	462	16	7	133.3
ATBSB	3100	Connate / 24.4%	4359	200	18	1	126.9
ATBST	2800	Smart / 0.69%	2097	113	17	6	67.8
ATBST	3500	Injection / 6.9%	2583	292	20	8	57.6
ATBST	3800	Connate / 24.4%	2390	420	12	6	81.5
ATBS8A	2500	Smart / 0.69%	306	49	12	3	4.1
ATBS8A	3500	Injection / 6.9%	265	42	10	3	3.6
ATBS8A	3600	Connate / 24.4%	287	55	11	5	4.5
ATBS8B	2200	Smart / 0.69%	209	30	5	2	3.6
ATBS8B	2700	Injection / 6.9%	124	15	5	3	1.4
ATBS8B	2900	Connate / 24.4%	36	23	3	2	0.4
AMNVPATBS1	3500	Smart / 0.69%	438	410	238	3	1.3
AMNVPATBS1	4400	Injection / 6.9%	17.4	3.2	1.0	0.7	0.1
AMNVPATBS1	4500	Connate / 24.4%	8.6	3.1	0.9	0.7	0.1
NVP1	7000	Smart / 0.69%	864	633	368	186	3.5
NVP1	9000	Injection / 6.9%	839	570	350	149	3.7
NVP1	9100	Connate / 24.4%	689	197	68	31	5.0
HYASA	6000	Smart / 0.69%	635	436	247	126	2.6
HYASA	8000	Injection / 6.9%	633	371	236	23	2.2
HYASA	7000	Connate / 24.4%	634	157	59	19	5.4
HYASB	6000	Smart / 0.69%	519	432	258	57.5	3.3
HYASB	8000	Injection / 6.9%	90.1	56.0	25.0	5.0	0.8
HYASB	6500	Connate / 24.4%	21.0	4.6	2.2	0.8	0.3
SG1	920	Smart / 0.69%	50	0.3	0.2	0.2	2
SG1	950	Injection / 6.9%	20	2	0.2	0.2	1
SG1	880	Connate / 24.4%	20	2	0.2	0.2	1

Table 5—Correlation coefficients from fits to Equations 1 and 2.

Polymer	Water / TDS	120ºC Eq .1	140ºC Eq .1	160ºC Eq .1	180ºC Eq .1	99°C Projection Eq. 2
ATBSA	Smart / 0.69%	0.807	0.947	0.968	0.984	0.999
ATBSA	Injection / 6.9%	0.836	0.928	0.988	0.980	0.998
ATBSA	Connate / 24.4%	0.810	0.904	0.792	0.595	0.965
ATBSB	Smart / 0.69%	0.585	0.833	0.959	0.959	0.977
ATBSB	Injection / 6.9%	0.749	0.919	0.903	0.968	0.982
ATBSB	Connate / 24.4%	0.712	0.476	0.888	0.981	0.964
ATBST	Smart / 0.69%	0.769	0.806	0.894	0.862	0.996
ATBST	Injection / 6.9%	0.744	0.906	0.904	0.979	0.988
ATBST	Connate / 24.4%	0.671	0.854	0.846	0.857	0.965
ATBS8A	Smart / 0.69%	0.987	0.989	0.987	0.997	0.999
ATBS8A	Injection / 6.9%	0.982	0.978	0.910	0.998	0.999
ATBS8A	Connate / 24.4%	0.972	0.990	0.843	1.000	0.999
ATBS8B	Smart / 0.69%	0.976	0.979	0.997	0.999	0.996
ATBS8B	Injection / 6.9%	0.942	0.971	0.979	0.633	0.985
ATBS8B	Connate / 24.4%	0.727	0.797	0.790	1.000	0.939
AMNVPATBS1	Smart / 0.69%	0.831	0.804	0.753	0.993	0.990
AMNVPATBS1	Injection / 6.9%	0.976	0.993	0.726	0.922	0.996
AMNVPATBS1	Connate / 24.4%	0.967	0.990	0.941	0.891	0.997
NVP1	Smart / 0.69%	0.749	0.831	0.925	0.876	0.980
NVP1	Injection / 6.9%	0.808	0.833	0.822	0.686	0.974
NVP1	Connate / 24.4%	0.589	0.832	0.852	0.917	0.998
HYASA	Smart / 0.69%	0.822	0.827	0.921	0.861	0.987
HYASA	Injection / 6.9%	0.838	0.809	0.731	0.959	0.903
HYASA	Connate / 24.4%	0.725	0.952	0.920	0.955	0.996
HYASB	Smart / 0.69%	0.795	0.806	0.928	0.962	0.903
HYASB	Injection / 6.9%	0.917	0.921	0.750	0.755	0.954
HYASB	Connate / 24.4%	0.875	0.624	0.989	0.953	0.976
SG1	Smart / 0.69%	0.977	1.000	1.000	1.000	0.825
SG1	Injection / 6.9%	0.978	0.982	1.000	1.000	0.953
SG1	Connate / 24.4%	0.953	0.911	1.000	1.000	0.932

Coreflood Results

Polymer Retention. Figure 4 shows the results of the polymer retention studies for the six anaerobic corefloods at 99°C. The cores were initially saturated with only injection water (6.8975% TDS, no oil).

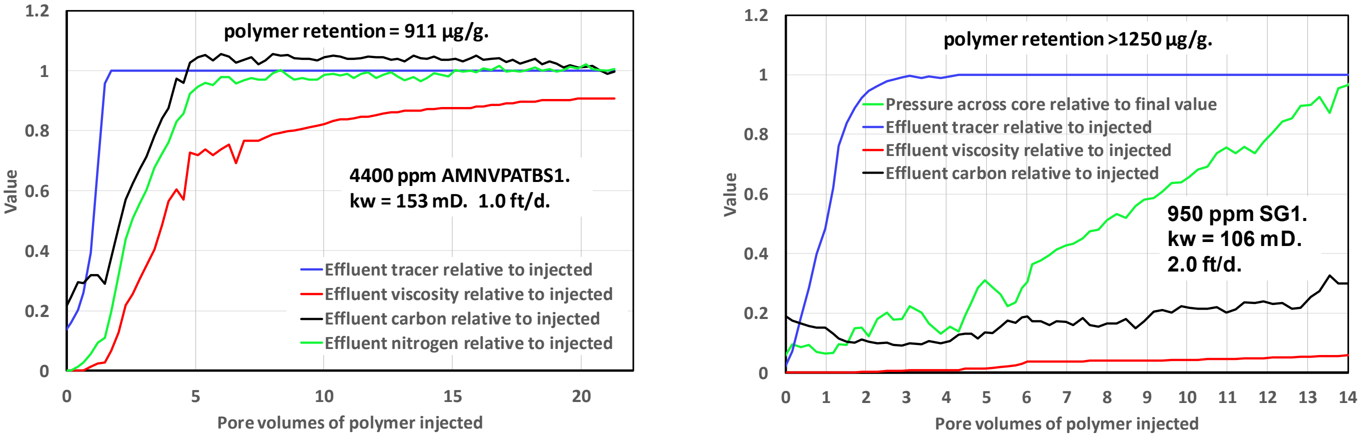

(a) AMNVPATBS1 in 153-mD carbonate

(d) SG1 scleroglucan in 106-mD carbonate

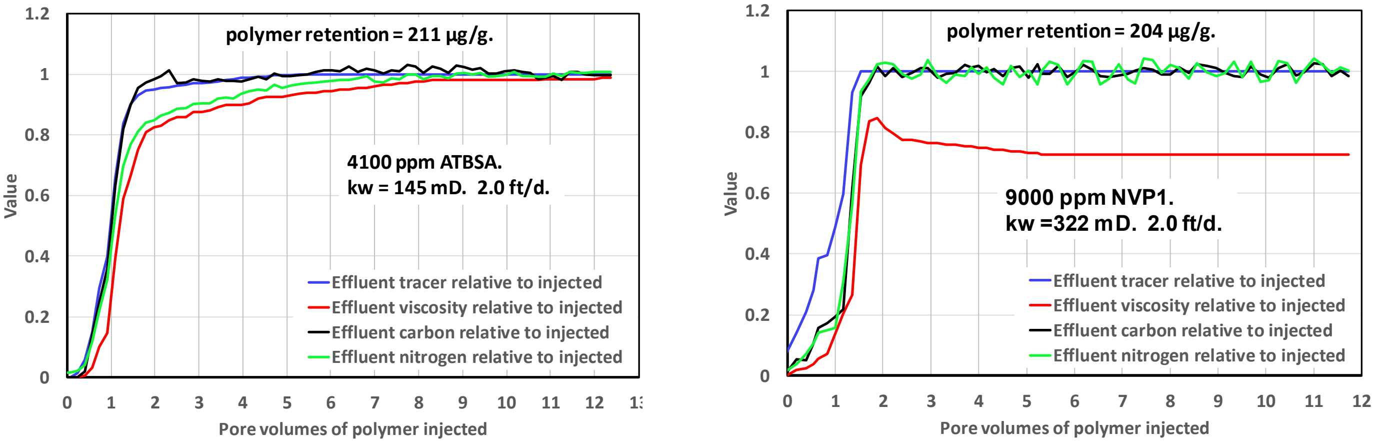

(b) ATBSA in 145-mD carbonate

(e) NVP1 in 322-mD carbonate

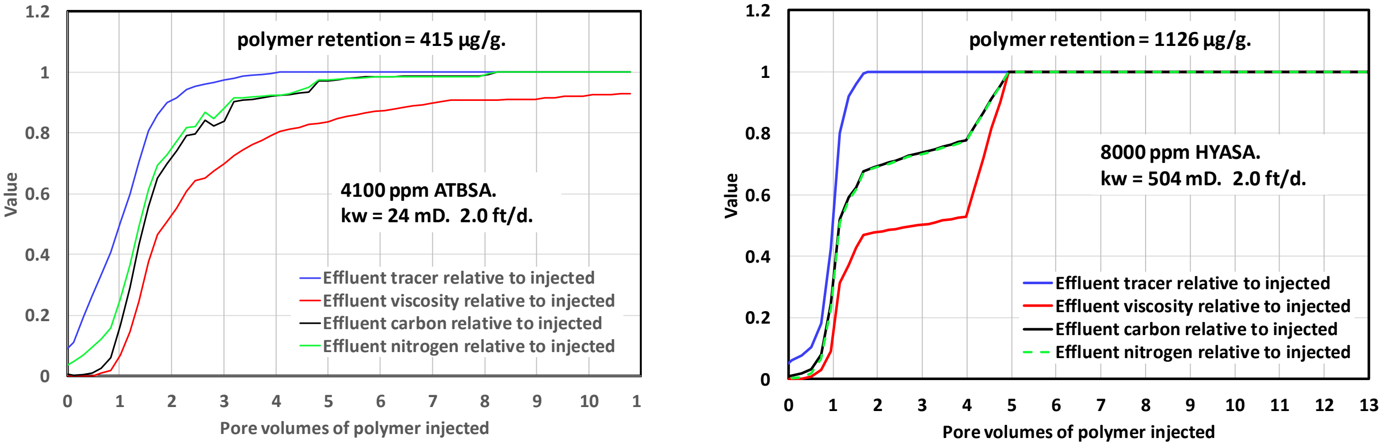

(c) ATBSA in 24-mD carbonate

(f) HYASA in 504-mD carbonate

Figure 4—Polymer retention results. 99°C. Injection water (6.8975% TDS). Anaerobic conditions.

Polymer retention was assessed using the methodology described in Manichand and Seright (2014) and Wang *et al*. (2020). Basically, polymer retention derives from the difference in area between the breakout curves for tracer (blue curves in Figure 4) and polymer (black, green, and red curves). In Figure 4, the black curves are effluent carbon (from TOC analysis), the green curves (except for scleroglucan) are effluent nitrogen (from chemiluminescent nitrogen), and the red curves are effluent viscosity (measured using a Vilastic VE rheometer at 25°C, 7.3 s^{-1}). For reasons described in Wang *et al*. (2020), inaccessible pore volume was zero, and the nitrogen curves were the most reliable indicator of effluent polymer concentration. (As an exception, since scleroglucan does not contain nitrogen, effluent carbon was used instead. In Figure 4d, the green curve indicates pressure drop across the core.) Polymer retention values are given in Figure 4 and also listed in Table 6. Calculated polymer retention values were 211 µg/g for ATBSA in 145-mD carbonate, 415 µg/g for ATBSA in 24-mD carbonate, 204 µg/g for NVP1 in 322-mD carbonate, 911 µg/g for AMNVPATBS1 in 153-mD carbonate, 1126 µg/g for HYASA in 504-mD carbonate, and more than 1250 µg/g for SG1 scleroglucan in 106-mD carbonate. As will be discussed later, these are all considered high retention values.

Table 6—Summary of anaerobic core flooding results at 99°C in carbonate cores.

Polymer	AMNVPATBS1	ATBSA	ATBSA	SG1	NVP1	HYASA
Core	272	28	15	264	24	324
Permeability, md	153	145	24	106	322	504
Concentration, mg/L	4400	4100	4100	950	9000	8000
Retention, µg/g	911	211	415	>1250	204	1126
Plugging observed while injecting?	no	no	no	yes	no	no
Resistance factor at 1-2 ft/d	28.4*	34	56	plugs	28.6	24.3
Initiial viscosity, cp @ 7.3 s^{-1}	20.8	21.0	22.6	34.8	20.6	26.7
Viscosity loss while injecting at 1-2 ft/d	9%	1%	7%	70%	23%	1%
Onset of mechanical degradation, ft/d	35	44	5	none	none	none
Onset of shear thickening, ft/d	9	11	1.3	none	66	53
Residual resistance factor	2.2	2.2	6.5	176	4	2.3

*1 ft/d for this flood. 2 ft/d for the others.

Plugging During Polymer Injection. Except for the case with scleroglucan (Figure 4d), pressures stabilized quickly (within 2 PV) during polymer injection. Thus, no progressive plugging was noted during most corefloods. In contrast, the green curve in Figure 4d reveals that injection pressure rose continuously during injecton of 14 PV of SG1 scleroglucan. After 14 PV, the effluent viscosity was only 6% of the injected value, while the effluent carbon was only 30% of the injected value. These results indicated very slow propagation of the SG1 polymer during the flood. As mentioned earlier, the calculated retention value exceeded 1250 µg/g. At the end of the experiment, a thick layer of slimy gel was noted on the injection face (Figure 5)—indicating the polymer was stripped from solution at the injection face. The polymer was dissolved very well prior to injection. There was no undissolved polymer (as was true for all six corefloods).

Figure 5—SG1 gel on the injection face at the end of the coreflood.

Resistance Factors. Resistance factor is defined as brine mobility (before polymer injection) divided by polymer-solution mobility. It is a measure of the effective viscosity of the polymer solution in porous media (relative to water). The seventh row in Table 6 lists stabilized resistance factors during the retention experiments of Figure 4. For comparison, the eighth row lists initial viscosity (at 25°C, 7.3 s^{-1}). For the cases of AMNVPATBS1, ATBSA in 145-mD rock, NVP1, and HYASA, resistance factors were roughly similar to the initial viscosity listing. This observation also suggests that little or no plugging (either on the face or internally within the core) occurred for these cases. For the case of ATBSA in 24-mD rock, the resistance factor (56) was 2.5 times greater than the viscosity listing—suggesting that some level of plugging occurred. For the case of SG1 scleroglucan, no resistance factor was calculated because severe face plugging was noted.

Viscosity Losses During Injection During Retention Experiments. Near the end of each retention experiment in Figure 4, we noted the fractional loss of viscosity upon propagation through the cores. As indicated in the ninth row of Table 6, these losses were modest or small (i.e., 1-9% loss) for AMNVPATBS1, ATBSA (in both permeabilities), and HYASA. For NVP1, the loss was 23%, which seems high considering that NVP polymers were thought to be very stable (Doe *et al.* 1987). However, our observations during the long-term stability study also noted relatively rapid loss of part of the NVP solutions viscosities at elevated temperatures. For SG1 scleroglucan, the effluent viscosity was only 6% of the injected value—due to stripping of the polymer from solution (as mentioned above).

Rheology and Mechanical Degradation In Porous Media. After the retention test, the polymer solution was injected at a sequence of rates to examine mechanical degradation and rheology in porous media. Figures 6 and 7 show the results. At the highest rate (139 ft/d) for AMNVPATBS1 (black curves in Figures 6 and 7), the resistance factor was 29.6 and the effluent viscosity was 33% less than the injected value (largely due to mechanical degradation). As rate was decreased to 8.7 ft/d, resistance factor decreased to 13.7. For rates of 34 ft/d and lower, the effluent viscosity was consistently 9% less than the injected value (attributed to thermal degradation). As rates decreased below 8.6 ft/d, resistance factors increased (to 59.8 at 1 ft/d). During this part of the experiment, the resistance factor at 1 ft/d (59.8) was significantly greater than the value (28.4) observed during the retention experiment. This result suggests some plugging occurred over the course of the rheology/mechanical-degradation part of the experiment. Overall, the black curves in Figures 6 and 7 suggest that in 153-mD rock, the onset of shear thickening occurred about 9 ft/d, and the onset of mechanical degradation occurred between 35 and 70 ft/d.

At the highest rate (88 ft/d) for ATBSA in 145-mD rock (solid red curves in Figures 6 and 7), the resistance factor was 53.5 and the effluent viscosity was 5% less than the injected value. As rate was decreased to 11 ft/d, resistance factor decreased to 17.4. For rates of 44 ft/d and lower, no significant degradation was apparent. As rates decreased below 11 ft/d, resistance factors increased (to ~24 at 1-2 ft/d). During this part of the experiment, the resistance factor at 2 ft/d (~24) was somewhat less than the value (34) observed during the retention experiment. No explanation is apparent for the difference. Overall, the red curves in Figures 6 and 7 suggest that in 145-mD rock, the onset of shear thickening occurred about 11 ft/d, and the onset of mechanical degradation occurred between 44 and 88 ft/d.

At the highest rate (10.6 ft/d) for ATBSA in 24-mD rock (red curves with red circles in Figures 6 and 7), the resistance factor was 81.8 and the effluent viscosity was 14% less than the injected value. As rate decreased to 1.3 ft/d, resistance factor decreased to 55.9. For rates of 2.6 ft/d and lower, no significant degradation was apparent. As rates decreased below 1.3 ft/d, resistance factors were fairly constant. During this part of the experiment, the resistance factor at 2 ft/d (~56) was roughly the same the value (59.6) observed during the retention experiment. Overall, the results suggest that in 24-mD rock, the onset of a very modest shear thickening occurred at about 1.3 ft/d, and the onset of mechanical degradation occurred at about 5 ft/d.

At the highest rate (280 ft/d) for SG1 scleroglucan (green curves in Figures 6 and 7), the resistance factor was 15.1 and the effluent viscosity was the same as the injected value. As rate was decreased to 70 ft/d, resistance factor increased to 43.7. Over this range, the effluent viscosity was the same as the injected value—indicating no mechanical degradation and that the polymer could propagate through the core at these high rates. For lower rates, the apparent shear thinning behavior continued, but the effluent viscosity decreased as rates were reduced below 18 ft/d—indicating the polymer was filtered from solution at the lower rates. The extremely high resistance factors at the lowest rates (3300 at 0.55 ft/d) were due to face plugging—not the actual rheology in porous media. Thus, in agreement with previous work at low temperatures, scleroglucan shows shear thinning rheology in porous media. At 99°C, the polymer propagates effectively and shows shear thinning behavior in the carbonate cores at high rates. However, at moderate and low rates at 99°C, SG1 scleroglucan plugs the carbonate rock.

At the highest rate (528 ft/d) for NVP1 (blue curves in Figures 6 and 7), the resistance factor was 14.9 and the effluent viscosity was the same as than the injected value. Thus, no mechanical degradation was noted, even at this very high rate. As rate was decreased to 66 ft/d, resistance factor decreased to 3.7—indicating that the onset of a mild shear thickening occurred at ~66 ft/d. As rates decreased from 66 to 4 ft/d, resistance factors were fairly similar (averaging about 4)—although an odd “hump” appears for the blue curve of Figure 6 with a peak at 16 ft/d. This is due to a single data point and may not be a real effect. As rates were further reduced to 1 ft/d, resistance factor increased to 17.3. At 9000-mg/L polymer, NVP1 required noticeably higher concentrations than the other polymers in providing viscosity and resistance factor. The blue curve in Figure 7 indicates increased viscosity loss as injection rate decreased. This behavior occurred because slower rates lead to longer exposure time (to 99°C), and therefore, greater thermal degradation at the slower rates. It was not due to mechanical degradation (because there was no viscosity loss at the highest rates), and it was not due to stripping of polymer (because the effluent nitrogen and carbon values were at the injected levels).

At the highest rate (846 ft/d) for HYASA (dashed black curves in Figures 6 and 7), the resistance factor was 11.3 and the effluent viscosity was the same as than the injected value. Thus, no mechanical degradation was noted, even at this very high rate. As rate was decreased to 53 ft/d, resistance factor decreased to 3.2—indicating that the onset of shear thickening occurred was around 53 ft/d in 504-mD rock. As rates decreased from 53 to 0.8 ft/d, resistance factors were fairly similar (averaging about 4). As rates were further reduced to 3.3 ft/d, resistance factor increased to 12.6. For lower rates (down to 0.2 ft/d) resistance factor remained fairly constant.

Residual Resistance Factors. Residual resistance factor is defined as brine mobility before polymer divided by brine mobility after polymer has been displaced. It is a measure of the permeability reduction caused by retention of a polymer. However, when no internal pressure taps are present (as in our experiments), any face plugging makes residual resistance factors appear artificially high. In our work, the experiment with SG1 scleroglucan showed obvious signs of face plugging (Figure 5). In the other corefloods, no polymer or gel was noted on the injection sand faces at the end of the experiments.

Previous work (Seright 2017, Wang *et al*. 2020) demonstrated that residual resistance factors may be artificially high if insufficient brine is flushed through the core. Specifically, more than 100 PV of brine may be required to displace all mobile polymer and achieve a true residual resistance factor.

For AMNVPATBS1, 134 PV of Injection brine was flushed through the core—yielding a final residual resistance factor of 2.2. These results might suggest a small amount of plugging—which is consistent with the observations associated with the 1-ft/d points discussed earlier for the black curve in Figure 6. For ATBSA, 79 PV of brine flush yielded a final residual resistance factors of 2.2 in 145-mD rock and 6.5 in 24-mD rock. With SG1 scleroglucan, 102 PV of brine flush resulted in a final residual resistance factor of 176—indicating a substantial amount of face plugging. After 79 PV of brine the final residual resistance factor was 4.0 for NVP1. For HYASA, flushing with 78 PV of brine was ended with a final residual resistance factor of 2.3.

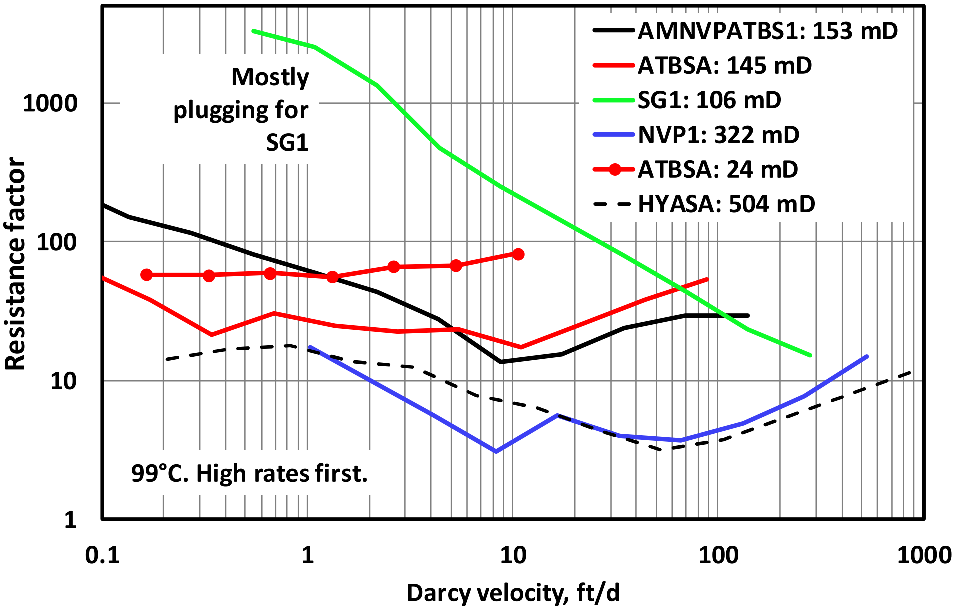

Figure 6—Resistance factors versus Darcy velocity for polymers in anaerobic carbonate cores at 99°C.

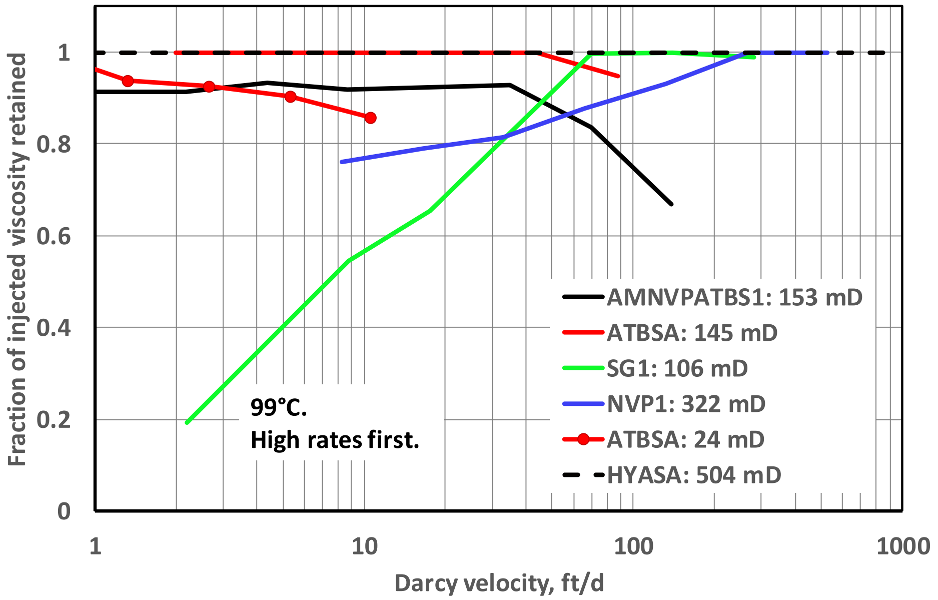

Figure 7—Viscosity losses after injection for polymers in anaerobic carbonate cores at 99°C.

Discussion

Long-Term Stability Discussion

HPAM (HPAM6). Partially hydrolyzed polyacrylamides (HPAM) are the most cost-effective polymer for low-salinity, low-temperature applications. Unfortunately, the literature indicates no hope that these polymers will be sufficiently stable at 99°C in the field Connate or Injection waters—because they will hydrolyze and precipitate. Some hope was held out that HPAM might be stable in the Smart water—even though the criteria from Moradi-Araghi and Doe (1987) indicated that the brine must not contain more than 135-mg/L calcium and 135-mg/L magnesium at our target temperature. (Smart water contains 288-mg/L calcium.) Consequently, tests were performed with HPAM6 (a common commercial HPAM with a Mw of 18 million g/mol and 30% degree of hydrolysis) (1600-mg/L, 25 cp at 7.3 s^{-1}, 25°C) to make sure.

Results confirmed that the HPAM precipitated quickly at elevated temperatures (less than 3 days at 120°C), even in Smart water. The precipitate was seen as a white layer at the bottom of the storage container. Total organic carbon analysis (Shimadzu TOC-Vcsh) confirmed that over 80% of the polymer precipitated from solution. Total nitrogen analysis (Shimadzu TOC-Vcsh) revealed that the ammonia that emanated from the HPAM remained free in solution. These results confirm that no HPAM will be sufficiently stable in any of the three field brines at elevated temperatures. The only way to make HPAM sufficiently stable is to remove divalent cations (especially calcium) from the waters to achieve a calcium concentration below 135 mg/L (from Moradi-Araghi and Doe 1987).

Acrylamide-ATBS Copolymer (AAMPS1). To reduce the hydrolysis/precipitation problem mentioned above, copolymers of acrylamide and ATBS (or AMPS) were proposed. An acrylamide-ATBS copolymer (AAMPS1) with a molecular weight of 6-8 million g/mol and 25% AMPS was obtained. For such chemistry, the ATBS monomer is slightly more expensive than acrylamide, and incorporation of ATBS does not allow achieving molecular weights as high as for HPAM. Consequently, ATBS copolymers usually require more polymer to achieve a given viscosity. The stability of AAMPS1 was studied in the three field brines at temperatures ranging from 120-180ºC. Initial solutions were clear. White precipitates were noted after a few days in all brines stored at temperatures of 140ºC or above. A white precipitate was also noted in the Connate water after 6 days at 120ºC. Significant viscosity losses occurred for all brines at all temperatures. TOC analysis confirmed loss of polymer from solution. The work of Sandengen *et al.* (2017) and Moradi-Araghi and Doe (1987) projects that the hydrolysis and precipitation problem will eventually occur at 99ºC for acrylamide-ATBS polymers with less than 40-50% ATBS, which is the case for the brines under consideration here. Since AAMPS1contains only 25% ATBS, it does not appear that this polymer will have sufficient stability for use in high-temperature, high-salinity, large-spacing applications. Because of (a speculated) concern of a major change in degradation mechanism between 100°C and 120°C, the stability of AAMPS1 was examined specifically at 99°C. The red curves in Figure 8 illustrate poor stability of AAMPS1 in the two most saline field brines at 99°C. At Day 50, it was already apparent that AAMPS1 gelled and was not sufficiently stable at 99°C in Connate water.

Scleroglucan (SG1). Scleroglucan is a neutral extracellular polysaccharide produced by the fungus Athelia (Sclerotium) rolfsii. The polysaccharide shares the backbone chemical structure of polymerized glucose. Its chemical structure consists of a linear β(1-3) D-glucose backbone, with one β(1-6) D-glucose side chain every three main residue. This polymer shares much in common with schizophyllan. Scleroglucan is suggested to have a triple-helix structure in solution—thus hopefully shielding the polymers from chemical attack and increasing stability over other polysaccharides (Fournier *et al*. 2018).

In the three brines (Smart, Injection, Connate), fits of the Arrhenius equation to the 120ºC and 140ºC scleroglucan-viscosity-loss data projected a viscosity half-life of about one year at 99ºC. The projection fits well with the actual behavior observed in Injection water at 99°C (blue curve in Figure 8a). The polymer is interesting in that only 880-950 mg/L of polymer are needed in the three brines to achieve the target viscosity (~25 cp). During our stability experiments at the highest temperatures (160-180°C), some of this scleroglucan biopolymer appeared to be "cooked" to a black residue. It is possible that this cooked material was cellular debris (associated with the fermentation process) that was not actually scleroglucan. Other than a small loss due to cooking of the polymer, the TOC analysis indicated that the polymer stayed in solution, regardless of the salinity or hardness of the brine.

As mentioned in the literature review, Davidson and Mentzer (1982), Kalpakci *et al.* (1990), and Jensen *et al.* (2018) reported good stability for scleroglucan in seawater at temperatures up to 100°C over a one-two year period, while Ryles (1988) noted that scleroglucan degraded within three months at 90°C. In view of these reported results, our stability experiments for scleroglucan were repeated. The replicate results basically confirmed that the polymer showed poor stability at 140°C and above. Scleroglucan showed a half-life of about 20 days at 120°C.

Because of (a speculated) concern of a major change in degradation mechanism between 100°C and

120°C, the stability of SG1 was studied specifically at 99°C. The blue curve in Figure 8a reveals that SG1 in Injection water exhibited a viscosity half-life of about one year (consistent with our earlier Arrhenius projection). In the Connate water (blue curve in Figure 8b), the polymer became gelatinous at 157 days at 99°C and was totally gelled at 437 days. Previous experience indicated that gelatinous polymers will not flow effectively through porous media. If these results and those of the above previous researchers are taken at face value, it appears that scleroglucan might exhibit good stability at 99°C in seawater (3-4% TDS) but not in our more saline brines (6.9-24.4% TDS).

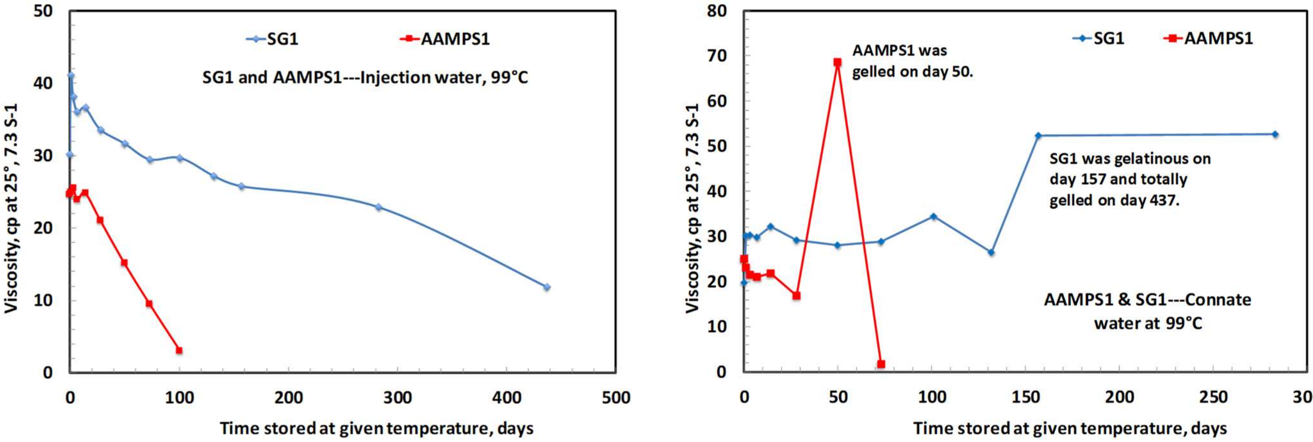

Figure 8—Stability of AAMPS1 and SG1 at 99°C in (a) Injection water (left) and (b) Connate water (right).

Polymers with High ATBS Content. Gaillard *et al.* (2015) provided generic compositions of polymers that contain acrylamide, acrylate, ATBS, and/or NVP. The polymers ATBSA, ATBSB, and ATBST contain very high ATBS levels. As of 621 days into the study, ATBSA exhibits excellent stability in all three brines at 120°C. In all three brines, the viscosity half-life was roughly 1 year at 140°C, 50 days at 160°C and about 8 days at 180°C. Substantial gel was noted in the Connate water after 84 days at 160°C. Achieving ~25 cp required 3100 mg/L in Smart water, 4100 mg/L in Injection water, and 4200 mg/L in Connate water.

Table 4 reveals that the polymers, ATBSB and ATBST, exhibit similar stability behavior as ATBSA. These three polymers all contain more than 90% ATBS. ATBSB has the same composition as ATBSA, but has a higher molecular weight—thus explaining why less polymer is needed to achieve the target viscosity (e.g., 2900 mg/L versus 4100 mg/L in Injection water). ATBST also has about the same composition as ATBSA, but it contains a small amount of a special monomer that reversibly promotes higher viscosities at high temperatures. All three polymers have over 90% degree of anionicity because the ATBS monomer is negatively charged. Also, one should note that the ATBS monomer has about three times the molecular weight of acrylamide (i.e., 207 versus 71 g/mol). Thus for a given degree of polymerization, an ATBS polymer has about three times higher molecular weight as polyacrylamide. For ATBSB, achieving ~25 cp required 2700 mg/L in Smart water, 2900 mg/L in Injection water, and 3100 mg/L in Connate water. For ATBST, achieving ~25 cp required 2800 mg/L in Smart water, 3500 mg/L in Injection Water, and 3800 mg/L in Connate water.

For the nine ATBS cases in Table 4, the projected half-lives at 99°C range from 55 to 133 years, with an average of 79 years and a standard deviation of 30 years. Note that all nine cases project a viscosity half-live exceeding 50 years at 99°C. For these same nine ATBS cases, the projected half-lives at 120°C averaged 5.6 years, with a standard deviation of 1.7 years. Within the uncertainty associated with the correlation coefficients in Table 5, it is unclear whether the three ATBS polymers have significantly different stabilities or that stability is different in the three brines. Stated another way, these three ATBS polymer exhibit excellent stability (i.e., the best ever reported for EOR polymers) at salinities ranging from 0.69% to 24.4% TDS and with divalent cation levels from 0.0342 to 2.16% (from Tables 1 and 4).

The study indicates that these three ATBS polymers should be sufficiently stable for potential applications with well spacings of 1-2 kilometers, where polymer stabilities of 17-34 years would be desired. However, in an effort to promote diversity of polymer vendors, only one of the three ATBS polymers was pursued during our coreflood studies.

In Table 4, the polymers labeled ATBS8A and ATBS8B are thought to contain around 80% ATBS. For the six ATBS8 cases in Table 4, the projected half-lives at 99°C range from 0.4 to 4.5 years, with an average of 2.9 years and a standard deviation of 1.6 years. The ATBS8 polymers were expected to be less stable than ATBSA, ATBSB, and ATBST, because they contain less ATBS (80% versus more than 90%). Within the uncertainty associated with the correlation coefficients in Table 5, it is unclear whether either of the ATBS8 polymers have significantly different stabilities or that stability is different in the three brines—although visually from the data, it appears that ATBS8A is more stable than ATBS8B, and the polymers are more stable in the less-saline brine (i.e., Smart water). Although these polymers may not be sufficiently stable for the more demanding high-temperature, high-salinity applications with large well spacing, they could be sufficiently stable for other applications that have tighter well spacing.

AMNVPATBS1 contained 50-65% acrylamide, 20-25% ATBS, and 5-20% NVP. For the three AMNVPATBS1 cases in Table 4, the projected half-lives at 99°C were 1.3 years in Smart water, but only 0.1 years in Injection water or Connate water. These findings are reasonably consistent with those reported by Gaillard *et al*. (2014) and Vermolen *et al*. (2011). It is doubtful that this polymer would be viable for the intended application. Nevertheless, this polymer was included during coreflood studies as a benchmark, because this polymer has been extensively studied internally—with some results reported by AlSofi *et al*. (2017). The decrease in stability from ATBS to ATBS8 to AMNVPATBS1 was expected because the ATBS content of the polymers decreased in that order.

N-Vinylpyrrolidone Polymer (NVP1). NVP1 is a powder-form polymer that contains a high level of N-vinylpyrrolidone (NVP). NVP1 solutions have generally remained clear, except that the solution in the Connate brine turned cloudy after 39 days at 180°C. In all three brines, the polymer solutions lost 40-60% of its original viscosity within two weeks at the tested temperatures. Also, the viscosity loss was greater as the storage temperature increased. We were surprised by this viscosity loss since NVP was expected to be a very stable monomer (Doe *et al*. 1987). After this initial viscosity loss, the decline in viscosity was much more gradual over the next 650 days at temperatures from 120°C to 160°C. In examining the statistics for NVP1, the projected half-life of the polymer is 3.5 to 5 years in the three brines (Table 4). However, the correlation coefficients are marginal for most NVP1 cases (Table 5). Because of the influence of the rapid initial viscosity loss, this skewed the fits for this polymer to give, perhaps, an overly pessimistic view of the polymer's stability. At 99°C, the polymer might be considerably more stable than indicated by the projections. At present, the primary concerns with this polymer are that 7000-9100-mg/L polymer is required to achieve the target viscosity and the polymer is thought to be quite expensive.

Gaillard *et al*. (2014) offered an explanation for the sudden viscosity loss, followed by more gradual degradation. They pointed out that during polymerization of NVP copolymers, the early part of the polymerization is dominanted by non-NVP monomers reacting first (producing polymers with low NVP content), while most of the NVP polymerization occurs later in the reaction. The implication is the fraction of the product that contained little NVP (e.g., acrylamide) is susceptible to rapid degradation and viscosity loss, while the material with high NVP content experiences much slower degradation.

Hydrophobic Associative Polymers (HYASA and HYASB). Solutions of HYASA lost viscosity at moderate rates, depending on the temperature. It showed similarities to NVP1 in that a significant viscosity loss occurred within the first two weeks, followed by a more gradual viscosity decline. The projected viscosity half-lives at 99°C were 2.6 and 2.2 years in Smart and Injection waters, respectively, but 5.4 years in Connate water (Table 4). As with NVP1, the correlation coefficients (Table 5) were not as high as for other polymers. So, the stability projections may be overly pessimistic. HYASB showed similar stability as HYASA in Smart water (3.3-year projected half-life at 99°C), but was notably less stable in the more saline brines. For HYASA, achieving ~25 cp required 6000 mg/L in Smart water, 8000 mg/L in Injection water and 7000 mg/L in Injection water. For HYASB, achieving ~25 cp required 6000 mg/L in Smart water, 8000 mg/L in Injection water and 6500 mg/L in Injection wate

Discussion of Coreflood Results

Retention. Table 6 provides a summary of the coreflood results. In these experiments, the lowest polymer retention value was 200 µg/g. For a 4100-ppm polymer solution, 200 µg/g requires that the polymer bank be increased in size by 13% to achieve the same effect as when no polymer retention occurs (Manichand and Seright 2014). Of course, polymer concentrations and retention values as high as some of those observed in this work could jolyeopardize the viability of a polymer flood. Note that our work was conducted in carbonate cores with no residual oil saturation present. Wever *et al*. (2018) observed that polymer retention was ten times lower at residual oil saturation than when no residual oil was present. In contrast, others (Wang *et al.* 2020) reported that retention was only modestly affected by the presence of residual oil. Future work will be performed to examine whether more palatable polymer retention values will occur under our conditions when residual oil is present. We acknowledge that the presence of residual oil may have an accentuated impact on retention of hydrophobic associative polymers.

Residual Resistance Factors and Plugging. Relatively short cores were available for this work (Table 3), so no internal pressure taps were used. Thus, if any face plugging occurred (whether immediate or prolonged), we could not distinguish face plugging from real resistance factors. Fortunately, for all but one of our floods, no continuous or sustained plugging occurred. Also, in three of the cases, residual resistance factors were low (~2), suggesting little face plugging (last row of Table 6). For two cases in Table 6, residual resistance factors ranged from 4 to 6.5—suggesting either that some face-plugging occurred or that some internal plugging of the core occurred. In these cases, we did not observe progressive plugging during polymer injection. The SG1 scleroglucan case was the only flood where severe progressive plugging was noted during polymer injection.

ATBSA. In 145-mD carbonate rock, ATBSA exhibited polymer retention of 211 µg/g, no plugging while injection, virtually no thermal degradation during injection at 1-2 ft/d, and a residual resistance factor of 2.2. In 24-mD carbonate, ATBSA exhibited polymer retention of 415 µg/g, no plugging during injection, 7% viscosity loss during injection at 1-2 ft/d, and a residual resistance factor of 6.5. As mentioned earlier, at 99°C, the projected viscosity half-life was over 50 years for this polymer.

Masalmeh *et al*. (2019) recently evaluated ATBSA at 105°C and 130°C in carbonate cores. Consistent with our results, they found the polymer showed good stability over six months at 130°C and over one year at 120°C. As in our experiments (Figure 6), they also noted shear thickening in porous media and good resistance to mechanical degradation. They reported polymer retention of 115 µg/g in a 263-mD carbonate core that was aged in the presence of crude oil. In cores with no oil, they found retention values of 316 µg/g in 121-mD carbonate, 209 µg/g in 45-mD carbonate, and 570 µg/g in 29-mD carbonate. These values are reasonably consistent with our value of 211 µg/g (measured with no residual oil saturation) in 153-mD carbonate.

Alfazazi *et al*. (2019) also examined ATBSA, at 25°C and 90°C in Indiana limestone cores. Most of their results were quite consistent with ours. Their retention values ranged from 194 to 340 µg/g in 143-153-mD carbonate—which brackets our value. They did report two differences in behavior. First, they reported no shear thickening for ATBSA at 90°C. Second, they noted a substantial degree of mechanical degradation. They suggested that the degradation might be attributable to passing through a back-pressure regulator.

Our results in 24-mD carbonate are also reasonably consistent with those reported by Masalmeh *et al.* (2019). In particular, our retention value of 415 µg/g in 24-mD carbonate is consistent with their value of 570 µg/g in 29-mD carbonate. In 44-mD carbonate, Hashmet *et al*. (2017) noted a residual resistance factor of 1.73 associated with a 0.1 PV polymer bank.

AMNVPATBS1. AMNVPATBS1 exhibited polymer retention of 911 µg/g, no plugging, a 9% viscosity loss during injection at 1-2 ft/d, and a residual resistance factor of 2.2. The projected viscosity half-lives at 99°C were 1.3 years in Smart water and 0.1 years in Injection water. In contrast to our polymer retention of 911 µg/g. Gaillard *et al*. (2014) reported retention of 84 µg/g for a similar polymer in carbonate cores under somewhat different conditions. For comparison, AlSofi *et al*. (2017b) reported HPAM retention values from 155 to 530 µg/g in carbonate cores at 99°C. Our AMNVPATBS1 residual resistance factor was 2.2. Gaillard *et al*. (2014) reported residual resistance factors for a similar polymer in the range of 1.1-1.3 in carbonate cores under somewhat different conditions. For comparison, HPAM and sulfonated polyacrylamide (containing ~25% ATBS) in seawater exhibited low residual resistance factors in carbonate cores at 99°C (Han *et al*. 2012 and AlSofi *et al*. 2017b).

SG1 Scleroglucan SG1 scleroglucan showed no mechanical degradation or shear thickening behavior at 99°C. However, it plugged the core during injection, exhibited polymer retention exceeding 1250 µg/g, and experienced a 70% viscosity loss while transiting the core at 1-2 ft/d.

Rivenq *et al*. (1992) reported scleroglucan retention of 30 µg/g at 90°C in a Berea sandstone core (in sea water). In NaCl solution, Audibert *et al*. (1993) also reported scleroglucan retention of 30 µg/g in Berea sandstone at 90°C. Fournier *et al*. (2018) reported retention of 8 µg/g in an Estaillade limestone core at 50°C. In contrast, Huang and Sorbie (1993) reported retention values over 80 µg/g (accompanied by apparent face plugging) in sand packs at room temperature. Kulawardana *et al*. (2012) found that scleroglucan propagated through Berea sandstone more rapidly (i.e., earlier arrival of the polymer front) as temperature increased from 25°C to 100°C. Although they did not report polymer retention values, examination of their data reveals that scleroglucan retention was quite high at 100°C. For schizophyllan (a polymer that is structurally similar to scleroglucan), Quadri *et al.* (2015a,b) reported low retention values (0.53-47.5 µg/g) in 3- to 165-mD carbonate cores at 120°C.

If the literature reports and our data are taken at face value, it appears that scleroglucan can show very good performance at high temperatures under some conditions of salinity (e.g., seawater), hardness, and core material, but not others. Under our particular conditions (6.9% TDS, 0.34% divalent cations, carbonate core), scleroglucan did not propagate well.

NVP1. NVP1 showed polymer retention of 204 µg/g, no mechanical degradation, and little or no plugging during injection, and a residual resistance factor of 4. However, the polymer experienced 23% viscosity loss during injection at 1-2 ft/d. This polymer required the highest concentration (9000 mg/L) to achieve the target viscosity. The projected half-life at 99°C was 3.7 years.

Doe *et al*. (1987) reported retention for this type of polymer in seawater at 121°C to be ~250 µg/g in ~100-mD Berea sandstone and ~100 µg/g in ~100-mD sandstone cores from the North Burbank unit (all at residual oil saturation).

HYASA. For HYASA at 99°C, the projected viscosity half-life ranged from 2.2 to 5.4 years, depending on the brine. This polymer exhibited a retention of 1126 µg/g, but no significant viscosity loss or plugging during flow through a 504-md carbonate core at 99°C. Residual resistance factor was 2.3. Reichenbach-Klinke *et al*. (2011) speculated that low residual resistance factors for polymers might indicate low polymer retention. However, results here and elsewhere (Wang *et al*. 2020) provide counter-examples to this idea.

Conclusions

An extensive evaluation was performed to identify polymers for use in polymer flooding high-temperature carbonate reservoirs with hard, saline brines. These polymers included new ATBS polymers, scleroglucan, NVP-based polymers, and hydrophobic associative polymers. The following conclusions resulted:

1. Three ATBS polymers were identified that were projected to provide a viscosity half-life over 50 years at 99˚C (under oxygen-free conditions) in the hard, saline brines of interest for the potential project. Other polymers examined in this study could not meet the required minimum of a 17-year half-life at 99˚C.
2. During corefloods using carbonate cores under oxygen-free conditions at 99˚C, polymer retention values were relatively high for all polymers examined—with the lowest values around 200 µg/g.
3. During the above corefloods, only scleroglucan exhibited significant plugging during injection of polymer solutions at 99˚C.
4. For all coreflood cases where plugging was not observed, resistance factors were consistent with expectations from viscosity measurements.
5. Three of five polymers showed modest or no viscosity loss in passing through cores at low velocity at 99˚C. As exceptions, one polymer (scleroglucan) showed substantial viscosity loss because of polymer being stripped from solution, while a synthetic NVP-based polymer experienced significant thermal degradation.
6. Residual resistance factors were moderate for cases where severe face plugging was not observed.

Nomenclature

A_1 = pre-exponential factor in Eq. 1, unit-less
A_2 = pre-exponential factor in Eq. 2, unit-less
C = polymer concentration, mg/L or ~ppm [µg/g]
E = Activation energy, cal/mol
k_w = absolute permeability to water, darcys [μm^2]
M_w = polymer molecular weight, g/mol [daltons]
PV = pore volumes of fluid injected
R = Universal gas constant, cal/mol
t = time, days
T = temperature, ˚K
μ = viscosity, cp [mPa-s]
μ_o = viscosity at time zero, cp [mPa-s]
μ_s = solvent viscosity, cp [mPa-s]
τ = decay constant, days
$\tau_{99^\circ C}$ = decay constant at 99˚C, days
ϕ = porosity

References

Alfazazi, U., AlAmeri, W., & Hashmet, M. R. 2018. Screening of New HPAM Base Polymers for Applications in High Temperature and High Salinity Carbonate Reservoirs. Paper SPE 192805 presented at the Abu Dhabi International Petroleum Exhibition & Conference held in Abu Dhabi, UAE, 12-15 November. http://dx.doi.org/10.2118/192805-MS.

Alfazazi, U., Thomas, N. C., AlAmeri, W., Al-Shalabi, E. W., and Shaik, A. R. 2019. An Experimental Investigation of Polymer Performance in Harsh Carbonate Reservoir Conditions. Paper 198607 presented at the SPE Gas & Oil Technology Showcase and Conference held in Dubai, UAE, 21-23 October. http://dx.doi.org/10.2118/198607-MS.

AlSofi, A. M., Wang, J., AlShuaibi, A. A., AlGhamdi, F. A., & Kaidar, Z. F. 2017a. Systematic Development and Laboratory Evaluation of Secondary Polymer Augmentation for a Slightly Viscous Arabian Heavy Reservoir. Paper SPE 183793 presented at the SPE Middle East Oil & Gas Show and Conference. Manama, Bahrain. 6-9 March. http://dx.doi.org/10.2118/183793-MS

AlSofi, A. M., Wang, J., Leng, Z., Abbad, M., and Kaidar, Z. F. 2017b. Assessment of Polymer Interactions with Carbonate Rocks and Implications for EOR Applications. Paper SPE 188086 presented at the SPE Kingdom of Saudi Arabia Annual Technical Symposium and Exhibition. Dammam, Saudi Arabia. 24-27 April. http://dx.doi.org/10.2118/188086-MS.

AlZahid, Y.A., AlBoqmi, A.M. and AlSofi, A.M., 2016, March. Toward an Alternative Bio-Based SP Flooding Technology:

II. Biopolymer Screening and Evaluation. SPE Paper 179746 presented at the SPE EOR Conference at Oil and Gas West Asia. Muscat, Oman. 21-23 March. http://dx.doi.org/10.2118/179746-MS.

Audibert, A., Noik, C., Lecourtier, J. 1993. Behavior of Polysaccharides under Harsh Conditions. *J. Canadian Petroleum Technology* **32**(7) 53-58.

Berge. A.B.G.M. Lenchenkov, N., Wever, D.A.Z., Farajzadeh, R. Al-Mjeni, R., and Glasbergen, G. 2018. The Role of Synthetic Polymer on Rock-Fluid Interactions and the Resulting Slug for a cEOR Flood in the Sultanate of Oman. Paper SPE 190391 presented at the SPE EOR Conference at Oil and Gas West Asia. Muscat, Oman. 26-28 March. http://dx.doi.org/10.2118/190391-MS.

Davison, P. and Mentzer, E. 1982. Polymer Flooding in North Sea Reservoirs. *SPE Journal* **22**(3): 353–362.

Delamaide, E. 2018. Polymers and Their Limits in Temperature, Salinity and Hardness: Theory and Practice. Paper SPE 192110 presented at the SPE Asia Pacific Oil & Gas Conference and Exhibition. Brisbane, Australia. 23-25 October. http://dx.doi.org/10.2118/192110-MS.

Divers, T., Gaillard, N., Bataille, S., Thomas, A., & Favéro, C. 2017. Successful Polymer Selection for CEOR: Brine Hardness and Mechanical Degradation Considerations. Paper 185418 presented at the SPE Oil and Gas Idia Conference and Exhibition. Mumbai, India 4-6 April. http://dx.doi.org/10.2118/185418MS.

Doe, P.H., Moradi-Araghi, A., Shaw, J.E., and Stahl, G.A. 1987. Development and Evaluation of EOR Polymers Suitable for Hostile Environments—Part 1: Copolymers of Vinylpyrrolidone and Acrylamide. *SPE Reservoir Engineering* **2**(4): 461467.

Dupuis, G., Antignard, S., Giovannetti, B., Gaillard, N., Jouenne, S., Bourdarot, G., … Zaitoun, A. (2017, November 13). A New Thermally Stable Synthetic Polymer for Harsh Conditions of Middle East Reservoirs. Part I. Thermal Stability and Injection in Carbonate Cores. Paper 188479 presented at the Abu Dhabi International Petroleum Exhibition & Conference. Abu Dhabi, UAE. 13-16 November. http://dx.doi.org/10.2118/188479MS.

Fournier, R., Tiehi, J. and Zaitoun, A. 2018. Laboratory Study of a New EOR-Grade Scleroglucan. Paper SPE 190451 presented at the SPE EOR Conference at Oil and Gas West Asia. Muscat, Oman. 26-28 March. http://dx.doi.org/10.2118/190451MS.

Gaillard, N., Giovannetti, B., and Favero, C. 2010. Improved Oil Recovery Using Thermally and Chemically Protected Compositions Based on Co and Terpolymers Containing Acrylamide. Paper SPE 129756 presented at the SPE Improved Oil Recovery Symposium. Tulsa, Oklahoma. 24-28 April. http://dx.doi.org/10.2118/129756MS.

Gaillard, N., Giovannetti, B., Favero, C., Caritey, J.P., Dupuis, G., & Zaitoun, A. 2014. New Water Soluble Anionic NVP Acrylamide Terpolymers for Use in Harsh EOR Conditions. Paper SPE 169108. Presented at the SPE Improved Oil Recovery Conference. Tulsa, Oklahoma. 12-16 April. http://dx.doi.org/10.2118/169108MS.

Gaillard, N., Giovannetti, B., Leblanc, T., Thomas, A., Braun, O., & Favero, C. 2015. Selection of Customized Polymers to Enhance Oil Recovery from High Temperature Reservoirs. Paper SPE 177073 presented at the SPE Latin American and Caribbean Petroleum Engineering Conference. Quito, Ecuador. 18-20 November. http://dx.doi.org/10.2118/177073MS.

Han, M., Zhou, X., Fuseni, A. B., Al-Zahrani, B. H., & AlSofi, A. M. 2012. Laboratory Investigation of the Injectivity of Sulfonated Polyacrylamide Solutions into Carbonate Reservoir Rocks. Paper SPE 155390 presented at the SPE EOR Conference at Oil and Gas West Asia. Muscat, Oman. 16-18 April. http://dx.doi.org/10.2118/155390-MS.

Hashmet, M. R., Qaiser, Y., Mathew, E. S., AlAmeri, W., & AlSumaiti, A. M. (2017, June 1). Injection of Polymer for Improved Sweep Efficiency in High Temperature High Salinity Carbonate Reservoirs: Linear X-Ray Aided Flood Front Monitoring. Paper 188125 prestented at the SPE Kingdom of Saudi Arabia Annual Technical Symposium and Exhibition. Dammam, Saudi Arabia. 24-27 April. http://dx.doi.org/10.2118/188125-MS.

Huang, Y. and Sorbie, K.S. 1993. Scleroglucan Behavior in Flow Through Porous Media: Comparison of Adsorption and In-Situ Rheology with Xanthan. Paper SPE 25173 presented at the Internationsl Symposium on Oilfield Chemistry. New Orleans, Louisiana. 2-5 March. http://dx.doi.org/10.2118/25173-MS.

Jabbar, M. Y., Al Sowaidi, A., Al Obeidli, A., Willingham, T. W., Britton, C., Adkins, S., … Teletzke, G. F. 2017. Chemical Formulation Design in High Salinity, High Temperature Carbonate Reservoir for a Super Giant Offshore Field in Middle East. Paper SPE 188604 presented at the Abu Dhabi International Petroleum Exhibition. Abu Dhabi, UAE. 13-16 November. http://dx.doi:10.2118/188604-MS.

Jabbar, M., Xiao, R., Teletzke, G. F., Willingham, T., Al Obeidli, A., Al Sowaidi, A., … Li, Z. 2018. Polymer EOR Assessment Through Integrated Laboratory and Simulation Evaluation for an Offshore Middle East Carbonate Reservoir. SPE 193274 presented at the Abu Dhabi International Petroleum Exhibition. Abu Dhabi, UAE. 12-15 November. http://dx.doi:10.2118/193274-MS.

Jensen, T., Kadhum, M., Kozlowicz, B., Sumner, E.S., Malsam, J., Muhammed, F., and Ravikiran, R. 2018. Chemical EOR Under Harsh Conditions: Scleroglucan As A Viable Commercial Solution. Paper SPE 190216 presented at the SPE Improved Oil Recovery Conference, Tulsa, Oklahoma. 1418 April. http://dx.doi.org/10.2118/190216-MS.

Jouenne, S., Klimenko, A., & Levitt, D. (2017, April 1). Polymer Flooding: Establishing Specifications for Dissolved Oxygen and Iron in Injection Water. *SPE Journal* **22**(2). 438-446 doi:10.2118/179614PA.

Kalpakci, B., Jeans, Y.T., Magri, N.F., and Padolewski, J.P. 1990. Thermal Stability of Scleroglucan at Realistic Rservoir Condtions. Paper SPE 20237 presented at the Symposium on Enhanced Oil Recovery. Tulsa, Oklahoma, 23-25 April. http://dx.doi.org/10.2118/20237-MS.

Kulawardana, E.U., Koh, H., Kim, D.H., Liyanage, P.J., Upamali, K.A.N., Huh, C., Weerasooriya, U., and Pope, G.A. 2012. Rheology and Transport of Improved EOR Polymers under Harsh Reservoir Conditions. Paper SPE 154294 presented at the SPE Improved Oil Recovery Symposium. Tulsa, Oklahoma. 14-18 April. http://dx.doi.org/10.2118/154294-MS.

Lake, L.W. 1989. Enhanced Oil Recovery. New Jersey, Prentice Hall: 396-400.

Leblanc, T., Braun, O., Thomas, A., Divers, T., Gaillard, N., & Favero, C. 2015. Rheological Properties of StimuliResponsive Polymers in Solution to Improve the Salinity and Temperature Performances of PolymerBased Chemical Enhanced Oil Recovery Technologies. Paper SPE 174618 presented at the SPE Enhanced Oil Recovery Conference. Kuala Lumpur, Malaysia. 11-13 April. http://dx.doi.org/10.2118/174618MS.

Leonhardt, B., Ernst, B., Reimann, S., Steigerwald, A., & Lehr, F. 2014. Field Testing the Polysaccharide Schizophyllan: Results of The First Year Paper SPE 169032 presented at the SPE Improved Oil Recovery Symposium. Tulsa, Oklahoma. 12-16 April. http://dx.doi.org/10.2118/169032-MS.

Maitin, B.K. 1992. Performance Analysis of Several Polyacrylamide Floods in North German Oil Fields. Paper SPE 24118 presented at the SPE/DOE Symposium on Enhanced Oil Recovery, Tulsa, Oklahoma, 22–24 April. http://dx.doi.org/10.2118/24118-MS.

Manichand, R.N., and Seright, R.S. 2014. Field vs Laboratory Polymer Retention Values for a Polymer Flood in the Tambaredjo Field. *SPE Res Eval & Eng*. **17**(3): 314-325 http://dx.doi.org/10.2118/169027-PA.

Masalmeh, S., AlSumaiti, A., Gaillard, N., Daguerre, F., Skauge, T., & Skuage, A. 2019. Extending Polymer Flooding Towards High-Temperature and High-Salinity Carbonate Reservoirs. Paper SPE 197647 presented at the Abu Dhabi International Petroleum Exhibition & Conference. Abu Dhabi, UAE, 11-14 November. http://dx.doi.org/10.2118/197647-MS.

Moradi-Araghi, A. and Doe, P.H. 1987. Hydrolysis and Precipitation of Polyacrylamide in Hard Brines at Elevated Temperatures. *SPE Reservoir Engineering* **2**(2): 189–198. http://dx.doi.org/10.2118/13033-PA.

Moradi-Araghi, A., Cleveland, D.H., Jones, W.W. and Westerman, I.J. 1987. Development and Evaluation of EOR Polymers Suitable for Hostile Environments: II: Copolymers of Acrylamide and Sodium AMPS. Paper SPE 16273 presented at the International Symposium on Oilfield Chemistry, San Antonio, Texas, 4–6 February. http://dx.doi.org/10.2118/16273-MS.

Nurmi, L., Sandengen, K., Hanski, S., & Molesworth, P. 2018. Sulfonated Polyacrylamides - Evaluation of Long Term Stability by Accelerated Aging at Elevated Temperature. Paper SPE 190184 Presented at the SPE Improved Oil Recovery Conference. Tulsa, Oklahoma. 14-18 April. http://dx.doi.org/10.2118/190184-MS.

Parker Jr., W.O., Lezzi, A., 1993. Hydrolysis of sodium2acrylamido2methylpropanesulfonate copolymers at elevated temperature in aqueous solution via 13C n.m.r. spectroscopy. *Polymer* **34** (23), 4913–4918. http://dx.doi.org/10.1016/0032-3861(93)90018-6.

Pope, G.A., Lake, L.W., and Helfferich, F. G. 1978. Cation Exchange in Chemical Flooding: Part 1—Basic Theory Without Dispersion. *SPE Journal 18*(6): 418-434. http://dx.doi.org/10.2118/6771-PA.

Quadri, S. M. R., Jiran, L., Shoaib, M., Hashmet, M. R., AlSumaiti, A. M., & Alhassan, S. M. 2015a. Application of Biopolymer to Improve Oil Recovery in High Temperature High Salinity Carbonate Reservoirs. Paper SPE 177915 presented at the SPE Abu Dhabi International Peroleum Exhibition and Conference. Abu Dhabi, UAE, 9-12 November. http://dx.doi.org/10.2118/177915-MS.

Quadri, S. M. R., Shoaib, M., AlSumaiti, A. M., & Alhassan, S. M. 2015b. Screening of Polymers for EOR in High Temperature, High Salinity and Carbonate Reservoir Conditions. International Petroleum Technology Conference. http://dx.doi.org/10.2523/IPTC-18436-MS.

Reichenbach-Klinke, R., Langlotz, B., Wenzke, B., Spindler, C., & Brodt, G. 2011. Associative Copolymer with Favorable Properties for the Application in Polymer Flooding. Paper 141107 presented at the SPE International Symposium on Oilfield Chemistry. The Woodlands, Texas. 11-13 April. http://dx.doi.org/10.2118/141107-MS.

Reichenbach-Klinke, R., Stavland, A., Langlotz, B., Wenzke, B., & Brodt, G. 2013. New Insights into the Mechanism of Mobility Reduction by Associative Type Copolymers. Paper SPE 165225 presented at the SPE Enhanced Oil Recovery Conference. Kuala Lumpur, Malaysia. 2-4 July. http://dx.doi.org/10.2118/165225-MS.

Reichenbach-Klinke, R., Zimmermann, T., Stavland, A., & Strand, D. 2018. Temperature-Switchable Polymers for Improved Oil Recovery. Paper 191317 presented at the SPE Norway One Day Seminar. Bergen, Norway. 18 April. http://dx.doi.org/10.2118/191317-MS.

Rivenq, R.C., Donche, A., and Noik, C. 1992. Improved Scleroglucan for Polymer Flooding Under Harsh Conditions. *SPE Reservoir Engineering* **7**(1) 15-20. SPE19635-PA. http://dx.doi.org/10.2118/19635-PA.

Rodriguez, L., Antignard, S., Giovannetti, B., Dupuis, G., Gaillard, N., Jouenne, S., … Grassl, B. 2018a. A New Thermally Stable Synthetic Polymer for Harsh Conditions of Middle East Reservoirs. Society of Exploration Geophysicists. http://dx.doi.org/10.1190/RDP2018-41754597.1.

Rodriguez, L, Antignard, S. Giovannetti, B., Dupuis, G., Gaillard, N., Jouenne, S., Bourdarot, G., Morel, D., Zaitoun, A. Grassi, B. 2018b. A New Thermally Stable Synthetic Polymer for Harsh Conditions of Middle East Reservoirs: Part II. NMT and Size Exclusion Chromotography t Assess Chemical and Structural Changes During Thermal Stability Tests. Paper SPE 190200. Presented at the SPE Improved Oil Recovery Conference. Tulsa, Oklahoma. 14-18 April. http://dx.doi.org/10.2118/190200-MS.

Ryles, R.G. 1988. Chemical Stability Limits of WaterSoluble Polymers Used in Oil Recovery. *SPE Reservoir Engineering* **3**(1): 23-34. http://dx.doi.org/10.2118/13585-PA.

Sandengen, K., Wideroe, H.C., Nurmi, L., Hanski, S. 2017. Hydrolysis Kinetics of ATBS Polymers at Elevated Temperatures via ^{13}C NMR Spectroscopy, as a Basis for Accelerated Aging Tests. *Journal of Petroleum Science and Engineering* **58**, 680-692. http://dx.doi.org/10.1016/j.petrol.2017.09.013.

Sandengen, K, Meldahl, M.M., Gjersvold, B., Molesworth, P. Gaillard, N., Braun, O., Antignard, S. 2018. Long Term Stability of ATBS Type Polymers for Enhanced Oil Recovery. *Journal of Petroleum Science and Engineering* **169**, 532-545. https://doi.org/10.1016/j.petrol.2018.06.001

Seright, R.S. and Henrici, B.J. 1990. Xanthan Stability at Elevated Temperatures. *SPE Reservoir Engineering* **5**(1): 52-60. http://dx.doi.org/10.2118/14946-PA.

Seright, R.S., Campbell, A.R., Mozley, P.S. and Han, P. 2010. Stability of PartiallyHydrolyzed Polyacrylamides at Elevated Temperatures in the Absence of Divalent Cations. *SPE Journal* **15**(2): 341-348. http://dx.doi.org/10.2118/121460-PA.

Seright, R.S., and Skjevrak, I. 2015. Effect of Dissolved Iron and Oxygen on Stability of HPAM. *SPE Journal* **20**(3): 433-441. http://dx.doi.org/10.2118/169030-PA.

Shupe, R.D. 1981. Chemical Stability of Polyacrylamide Polymers. *J. Pet. Tech.* **33**(8): 1513–1529. http://dx.doi.org/10.2118/9299-PA.

Siggel, L., Radloff, M., Reimann, S., Hansch, M., Nowak, M., Ranft, M., … Brand, F. 2014. TPM''s: A New Class of Viscoelastic Solutions for Enhanced Oil Recovery. Paper SPE 169689 presented at the SPE EOR Conference at Oil and Gas West Asia. Muscat, Oman. 31 March-2 April. http://dx.doi.org/10.2118/169689-MS.

Swiecinski, F., Reed, P., Andrews, W., 2016. The Thermal Stability of Polyacrylamides in EOR Applications. Paper SPE 179558 presented at the SPE Improved Oil Recovery Conference. Tulsa, Oklahoma. 11-13 April. http://dx.doi.org/10.2118/179558MS.

Vermolen, E. C. M., Van Haasterecht, M. J. T., Masalmeh, S. K., Faber, M. J., Boersma, D. M., & Gruenenfelder, M. A. 2011. Pushing the envelope for polymer flooding towards high-temperature and high-salinity reservoirs with polyacrylamide based terpolymers. Paper 141497 presented at the SPE Middle East Oil and Gas Show and Conference. Manama, Bahrain. 25-28 September. http://dx.doi.org/10.2118/141497MS.

Wever, D. A. Z., Bartlema, H., ten Berge, A. B. G. M., Al-Mjeni, R., & Glasbergen, G. 2018. The Effect of the Presence of Oil on Polymer Retention in Porous Media from Clastic Reservoirs in the Sultanate of Oman. Paper SPE 190430 presented at the SPE EOR Conference at Oil and Gas West Asia. Muscat, Oman. 26-28 March. http://dx.doi.org/10.2118/190430-MS.

Xu, T, White, S.P., Pruess, K., and Brimhall, G. 2000. Modeling Pyrite Oxidation in Saturated and Unsaturated Subsurface Flow Systems. *Transport in Porous Media* **39**: 25–56.

Yang, S.H. and Treiber, L.E. 1985. Chemical Stability of Polyacrylamide Under Simulated Field Conditions. Paper SPE 14232 presented at the SPE Annual Technical Conference and Exhibition, Las Vegas, Nevada, 22–25 September. http://dx.doi.org/10.2118/14232MS.

Wang, D., Seright, R.S., Shao, Z. et al. 2008. Key Aspects of Project Design for Polymer Flooding at the Daqing Oil Field. *SPE Res. Eval & Eng* **11** (6): 1117–1124. SPE-109682-PA. http://dx.doi.org/10.2118/109682-PA.

Wang, D., Dong, H., Lv, C. et al. 2009. Review of Practical Experience of Polymer Flooding at Daqing. *SPE Res. Eval & Eng* **12** (3): 470–476. SPE-114342-PA. http://dx.doi.org/10.2118/114342-PA.

Wang, D., Li, C., and Seright, R.S. 2020. Polymer Retention Evaluation in a Heavy Oil Sand for a Polymer Flooding Application on Alaska's North Slope. Paper SPE 200428 presented at the SPE Improved Oil Recovery Symposium. Tulsa, Oklahoma. 20-22 April. http://dx.doi.org/10.2118/200428MS.

Wassmuth, F.R., Green, K., Hodgins, L. et al. 2007. Polymer Flood Technology for Heavy Oil Recovery. Presented at the Canadian International Petroleum Conference, Calgary, Alberta, Canada, 12–14 June. PETSOC-2007-182. http://dx.doi.org/10.2118/2007-182.

Zaitoun, A. and Potie, B. 1983. Limiting Conditions for the Use of Hydrolyzed Polyacrylamides in Brines Containing Divalent Ions. Paper SPE 11785 presented at the International Symposium on Oilfield Chemistry, Denver, Colorado, 1–3 June. http://dx.doi.org/10.2118/11785MS.

Zhang, X., Han, M., Fuseni, A., & AlSofi, A. M. 2017. A New Facile Approach to Estimate EOR Polymers Thermal Stability at Harsh Reservoir Conditions. Paper 188909 presented at the Ahu Dhabi International Petroleum Exhibition & Conference. Abu Dhabi, UAE. 13-16 November. http://dx.doi.org/10.2118/188909-MS.

Zhuoyan, Z., Quan, X., Hanbing, X., Jian, F., Feng, W., Juedu, A., … Dehai, H. (2015, May 4). Evaluation of the Potential of HighTemperature, LowSalinity Polymer Flood for the Gao30 Reservoir in the Huabei Oilfield, China: Experimental and Reservoir Simulation Results. Paper OTC-25817 presented at the Offshore Technology Conference. Houston, Texas. 4-7 May. http://dx.doi.org/10.4043/25817MS.

SI Metric Conversion Factors

cp x 1.0*	E-03	= Pa·s
ft x 3.048*	E-01	= m
in. x 2.54*	E+00	= cm
mD x 9.869 233	E-04	= μm^2
psi x 6.894 757	E+00	= kPa

* Conversion is exact.

Author Biographies

Randy Seright is a Senior Engineer at the Petroleum Recovery Research Center of the New Mexico Institute of Mining and Technology, where he has worked the past 33 years. He has a BS degree in chemical engineering from Montana State University and a PhD degree in chemical engineering from the University of Wisconsin.

Kate Wavrik is a Research Associate IV at New Mexico Tech's Petroleum Recovery Research Center where she has worked for 17 years under the guidance of Dr. Seright. She has a BS in Petroleum and Natural Gas Engineering from New Mexico Institute of Mining and Technology (New Mexico Tech).

Guoyin Zhang is a Research Scientist and Section Head of Alkaline/Surfactant/Polymer Flooding group at the Petroleum Recovery Research Center (PRRC)/New Mexico Tech. He has a BS degree in applied chemistry from China University of Petroleum and a PhD degree in petroleum engineering from New Mexico Tech. Before joining the PRRC, he worked on chemical flooding for the Daqing Oilfield Company for 14 years.

Abdulkareem AlSofi is Chief Technologist at the EXPEC Advanced Research Center of Saudi Aramco, where he has worked since 2011. He has a BS in Petroleum Engineering from the University of Texas at Austin and a PhD in Petroleum Engineering from Imperial College London.